Technical Note: Preventing CO_2 overestimation from mercuric or copper (II) chloride preservation of dissolved greenhouse gases in freshwater samples

François Clayer[1*], Jan Erik Thrane[1], Kuria Ndungu[1], Andrew King[1], Peter Dörsch[2], Thomas Rohrlack[2]

[1]Norwegian Institute for Water Research (NIVA), Økernveien 94, 0579 Oslo, Norway

[2]Faculty of Environmental Sciences and Natural Resource Management, Norwegian University of Life Sciences, PO Box 5003, 1432 Ås, Norway

[*]Corresponding author(s): François Clayer (francois.clayer@niva.no)

Abstract

The determination of dissolved gases (O_2, CO_2, CH_4, N_2O, N_2) in surface waters allows to estimate biological processes and greenhouse gas fluxes in aquatic ecosystems. Mercuric chloride ($HgCl_2$) has been widely used to preserve water samples prior to gas analysis. However, alternates are needed because of the environmental impacts and prohibition of mercury. $HgCl_2$ is a weak acid and interferes with dissolved organic carbon (DOC). Hence, we tested the effect of $HgCl_2$ and two substitutes (copper (II) chloride – $CuCl_2$ and silver nitrate – $AgNO_3$), as well as storage time (24h to 3 months) on the determination of dissolved gases in low ionic strength and high DOC water from a typical boreal lake. Furthermore, we investigated and predicted the effect of $HgCl_2$ on CO_2 concentrations in periodic samples from another lake experiencing pH variations (5.4–7.3) related to *in situ* photosynthesis. Samples fixed with inhibitors generally showed negligible O_2 consumption. However, effective preservation of dissolved CO_2, CH_4 and N_2O for up to three months prior to dissolved gas analysis, was only achieved with $AgNO_3$. In contrast, $HgCl_2$ and $CuCl_2$ caused an initial increase in CO_2 and N_2O from 24h to 3 weeks followed by a decrease from 3 weeks to 3 months. The CO_2 overestimation, caused by $HgCl_2$-acidification and shift in the carbonate equilibrium, can be calculated from predictions of chemical speciation. Errors due to CO_2 overestimation in $HgCl_2$-preserved water, sampled from low ionic strength and high DOC freshwater that are common in the northern hemisphere, could lead to an overestimation of the CO_2 diffusion efflux by a factor of >20 over a month, or a factor of 2 over the ice-free season. The use of $HgCl_2$ and $CuCl_2$ for freshwater preservation should therefore be discontinued. Further testing of $AgNO_3$ preservation should be performed under a large range of freshwater chemical characteristics.

Key-words: lake, greenhouse gases, water sample preservation, mercuric chloride, metal toxicity, carbon dioxide

Running tile: CO_2 overestimation from $HgCl_2$ fixation

1 Introduction

The determination of dissolved gases by gas chromatography from water samples collected in the field allows the estimation of biological processes in aquatic ecosystems such as photosynthesis and oxic respiration (O_2, CO_2), denitrification (N_2, N_2O) and methanogenesis (CH_4). This technique is also useful to test the calibration of *in-situ* sensors in long term deployment. However, the accuracy of this approach largely depends on the effectiveness of sample fixation. In fact, the partial pressure of the dissolved gases will continue to evolve in the water sample from the time of collection to the time of analysis unless biological activity is prevented. This is an issue when field sites are far from laboratory facilities, and when samples need to be stored until the end of the field season for more efficient processing in large batches. Hence, before using a given chemical to preserve water samples, it must be ensured that it is efficient in inhibiting biological activity without changing the sample's chemistry.

Mercuric (II) chloride ($HgCl_2$) has been widely used as an inhibitor of the above-mentioned biological processes to preserve water samples for the determination of dissolved CO_2 in seawaters (e.g. Dickson, Sabine & Christian, 2007) and several dissolved gases in natural and artificial freshwater bodies (e.g. O_2, CO_2, CH_4, N_2 and/or N_2O; Guérin et al., 2006; Hessen et al., 2017; Hilgert et al., 2019; Okuku et al., 2019; Schubert et al., 2012; Xiao et al., 2014; Yan et al., 2018; Yang et al., 2015) because it proved effective at very low concentrations compared to other reagents (e.g. Horvatić & Peršić, 2007; Hassen *et al.*, 1998). Worldwide efforts have sought to reduce the use of mercury because it is considered toxic to the environment and exposure can severely affect human health (Chen et al., 2018). Therefore, alternative preservation techniques to $HgCl_2$ treatment have been tested for dissolved inorganic carbon (DIC) and δ^{13}C-DIC such as acidification with phosphoric acid (Taipale & Sonninen, 2009) or a combination of filtration and exposure to benzalkonium chloride or sodium chloride (Takahashi *et al.*, 2019). Previous studies showed that simple filtration (and cooling), fixation (precipitation) or acidification were effective in preserving water samples (Wilson, Munizzi & Erhardt, 2020). An alternative to using preservatives is to collect in-situ water samples, extract the headspace in the field, and analyze the headspace in a laboratory (e.g., Cole et al., 1994; Karlsson et al., 2013; Kling et al., 1991). However, these techniques were not tested for the simultaneous determination of several dissolved gases, including CH_4 which is subject to rapid degassing during handling or storage if samples are not preserved because of its low solubility in water (Duan & Mao, 2006). In addition, some of the existing alternatives, such as filtration or field headspace equilibration, are difficult to operate in remote areas in the field under harsh weather conditions and prone to potential ambient air contamination. Solutions for water sample preservation should therefore involve a minimum of manipulation steps in the field to avoid gas exchange with ambient air. Preservative amendments into sealed water bottles appears as one of the most efficient methods. Copper(II)

chloride ($CuCl_2$) and silver nitrate ($AgNO_3$), the most toxic form of silver, are relevant alternatives to $HgCl_2$ given their known toxicity (e.g., Ratte 2009; Amorim and Scott-Fordsmand 2012) and wide application in water treatments and water purification (Larrañaga et al., 2016; Nowack et al., 2011; NPIRS, 2023; Ullmann et al., 1985). Nevertheless, the efficiency of these alternative preservatives has never been tested for dissolved gas samples preservation.

The addition of $HgCl_2$ to water is known to produce hydrochloric acid through hydrolysis (Ciavatta & Grimaldi, 1968) and to form complexes with many environmental ligands, both inorganic (Powell *et al.*, 2004) and organic (Tipping, 2007; Foti *et al.*, 2009; Liang *et al.*, 2019; Chen *et al.*, 2017). The complexation of Hg^+ with the carboxyl or thiol groups of DOC in oxic environments could further increase the concentration of H^+ (Khwaja et al., 2006; Skyllberg, 2008). This acidification can be an issue in poorly buffered water (low ionic strength) with high concentration of DOC where a shift in the pH and carbonate equilibrium can be induced. In that case, the estimated CO_2 concentration would be higher after $HgCl_2$ fixation than the *in situ* concentration, and if the shift in pH is not accounted for, can result in an overestimation of dissolved CO_2 and bicarbonate concentrations. A similar acidification effect is also expected with $CuCl_2$ treatments (Rippner et al., 2021), but not for $AgNO_3$ treatments. Such effects would not be expected in marine water due to the high ionic strength of the water (Chou *et al.*, 2016) or freshwater with low pH (<5.5) under which conditions nearly all dissolved inorganic carbon is CO_2 (Stumm & Morgan, 1981). Thus, there are clear limits of the application of $HgCl_2$, and possibly $CuCl_2$, for freshwater sample preservation given its risk of leading to overestimation of CO_2 and bicarbonate concentrations, in addition to exposing field workers to the risks of its high toxicity.

Here we combine data from laboratory experiments (i) and field work (ii) to illustrate risks of mis-estimation of dissolved gas concentrations in freshwaters with some preservatives and provide recommendation for best practices in the field. First, we (i) performed some short-term and long-term incubations of water from a typical heterotrophic unproductive boreal lake with circumneutral pH, low ionic strength (poor buffering capacity) and high DOC concentration to test the effect of storage time and different preservative treatments on the determination of five dissolved gases (O_2, CO_2, CH_4, N_2 and N_2O) by headspace equilibration and gas chromatography. The preservatives were mercuric chloride ($HgCl_2$) and two alternative inhibitors, chosen for their wide and effective application in water treatments and water purification (copper (II) chloride – $CuCl_2$ and silver nitrate – $AgNO_3$; Xu & Imlay, 2012; Rai, Gaur & Kumar, 1981). Unamended water samples, where only ultrapure water was added, were also included for comparison. In addition, we (ii) analysed dissolved CO_2 concentration data obtained from a typical productive boreal lake using two independent methods, one by gas chromatography following $HgCl_2$ fixation, and one through dissolved inorganic carbon

determination without fixation. We show that the overestimation of dissolved CO_2 concentrations caused by $HgCl_2$ fixation can be predicted based on chemical equilibria.

2. Methods

The detailed experimental procedures for investigating (i) the effects of storage time and different inhibitors on dissolved gas concentrations as well as (ii) the effects of $HgCl_2$ on dissolved CO_2 analyses over a range of pH values are summarized in Fig. 1 and described below.

2.1. Effects of storage time and inhibitors on the quantification of dissolved gases

Study site and sampling

Surface water was collected from Lake Svartkulp (59.9761313 N, 10.7363544 E; Southeast Norway) north of Oslo, Norway, on the 4th of September 2019. A 5 L plastic bottle was gently pushed into the water and progressively tilted to let the water flow into the bottles without bubbling. The bottle aperture was covered with a 90 µm plankton net to avoid sampling large particles. This procedure was repeated five times to yield a total water volume of 25 L. The 5 L water bottles were immediately brought back to the lab. Upon arrival at the laboratory, after temperature equilibration, water from the 5 L bottles was slowly poured, to limit gas exchange with the ambient air, into a 25 L tank to provide a single bulk sample to start the incubation experiment. Filtration, e.g., with 0.45 or 0.2 µm filters, was avoided to minimize changes in dissolved gas concentrations (e.g., Magen et al., 2014). The mixed water sample (25 L) was sub-sampled (0.5 L) for the determination of alkalinity (127 µmol L^{-1}), pH (6.73), ammonium (3 µg N L^{-1}), nitrate (5 µg N L^{-1}), total N (230 µg N L^{-1}), phosphate (1 µg P L^{-1}), total P (9 µg P L^{-1}) and TOC (8.9 mg C L^{-1}) all analysed by standard methods at the accredited Norwegian Institute for Water Research (NIVA) lab (see Tab. S1). *In situ* temperature of the lake water was measured with a handheld thermometer and was 18.5 °C. Note that particulate organic carbon is a negligible fraction of TOC in Norwegian lake waters, representing on average less than 3% (de Wit et al., 2023).

Lake Svartkulp was selected for this experiment because it is representative of low ionic strength Northern Hemisphere lakes, typically found in granitic bedrock regions in North-East America and Scandinavia. It is a typical low-productivity, heterotrophic, slightly acidic to neutral, moderately humic lake. Similar lakes are found in Southern Norway (de Wit et al., 2023), large parts of Sweden (Valina et al. 2014), Finland, Atlantic Canada (Houle et al., 2022), Ontario, Québec, and North-East USA (Skjelkvåle and de Wit 2011; Weyhenmeyer et al., 2019).

Laboratory incubation experiment with different preservatives and storage times

The experimental design involved to incubate 72 borosilicate glass bottles (120 mL) filled with lake water from our 25 L bulk sample subjected to four different treatments: addition of 240µL of a preservative solution of (i) $HgCl_2$, (ii) $CuCl_2$ or a (iii) $AgNO_3$, or addition of 240 µL of (iv) MilliQ water. The bottles amended with MilliQ water are hereafter referred to as "unfixed". The 72 bottles were divided into three groups which were incubated cold (+4°C) and dark for 24h, three weeks or three months respectively, before being processed for dissolved gas analysis by gas chromatography. These incubation times were selected to represent situations where samples are processed directly upon return to the laboratory (24h), or after medium (3 weeks) to long (3 months) -term storage, respectively. At each time point and for each treatment, a group of 6 bottles were further processed for dissolved gas analysis. Concentrations of O_2, N_2, N_2O, CO_2 and CH_4 were determined by gas chromatography (see below) using the headspace technique following Yang *et al.* (2015). pH was not measured at the end of the storage period.

In details, within 3h of lake water sampling, the 120mL bottles were gently filled with water from the mixed sample (25 L). Each 120mL bottle was slowly lowered into the water and progressively tilted to let the water flow into the bottle without bubbling. The bottle was then capped under water with a gas tight butyl rubber stopper after ensuring that there were no air bubbles in the bottle. The bottles were randomized prior to preservative or MilliQ treatment. The preservative or MilliQ amendment was pushed in each bottle with a syringe and needle through the rubber septum. To avoid overpressure, another needle was placed through septum at the same time, at least 2 cm above the other needle, to allow an equivalent volume of clean water to be released.

Stock solutions of $HgCl_2$, $CuCl_2$ and $AgNO_3$ were prepared according to Tab. 1 using high accuracy chemical equipment (e.g., high accuracy scale, volumetric flasks). The Ag (Silver nitrate EMSURE® ACS; Merck KGaA, Germany) Cu (Copper(II) chloride dihydrate; Merck Life Science ApS, Norway) and Hg (Mercury(II) chloride; undetermined) salts were dissolved in MilliQ ultrapure water (>18 MΩ cm). For measurement of CO_2 in seawater samples, the standard method involves poisoning the samples by adding a saturated $HgCl_2$ solution in a volume equal to 0.05-0.02% of the total volume (Dickson 2007). We used this as a starting point and added 0.02 % saturated $HgCl_2$ solution to 18 bottles (240 µL of $HgCl_2$ 10× diluted saturated solution), resulting in a sample concentration of 14 µg $HgCl_2$ mL^{-1} (51.6 µM; Tab. 1). Based on estimated toxicity relative to Hg (Deheyn et al., 2004; Halmi et al., 2019), the silver and copper salts were added in molar concentrations equal to two and three times the molar concentration of $HgCl_2$, respectively (Tab. 1), although it varies between species of microorganisms and environmental matrices (Hassen *et al.*, 1998; Rai, Gaur & Kumar, 1981).

Additional 24h incubation experiment with different preservatives for pH measurements

Since pH was not measured at the end of the first incubation experiment, we performed an additional experiment to document any potential rapid (within 24h) impacts of preservative on pH. A total of 48

borosilicate glass bottles (120 mL) filled with lake water were subjected to the same four different treatments as the first experiment described above: $HgCl_2$, $CuCl_2$, $AgNO_3$ or MilliQ water amendments. To this end, a 20L water tank was filled with surface water from Lake Svartkulp on the 14th of December 2023. The water tank was immediately returned to the laboratory and left for 24h to equilibrate to the room temperature. On December 15th, 120mL bottles were gently filled with water from the bulk 20L sample, as described above. The bottles were randomized prior to preservative or MilliQ treatment performed as described above. The bottles were then incubated at room temperature for 2h or 24h. pH was measured in the initial unamended lake water, in 24 bottles opened after 2h incubation, and in 24 bottles opened after 24h incubation. pH measurements were performed with a WTW Multi 3620 pH meter calibrated using a two-point calibration at pH = 4 and pH = 7. All pH measures were corrected for temperature. Water temperature of the water samples during pH measurements ranged between 19.1 and 21.2°C.

2.2. Effects of $HgCl_2$ on dissolved CO_2 analyses over a range of pH values

Study site and sampling

Water samples were collected from Lake Lundebyvannet located southeast of Oslo (59.54911 N, 11.47843 E, Southeast Norway). Two sets of samples were taken from 1, 1.5, 2 and 2.5 m depth using a water sampler once or twice a week between April 2020 and January 2021 for the determination of (i) dissolved CO_2 by GC analysis following fixation with $HgCl_2$ and (ii) DIC analysis with a TOC analyser. Samples for GC analysis were filled into 120 mL glass bottles (as described above for the 72 incubation bottles), which were sealed with rubber septa under water without air bubbles. Samples for GC analysis were preserved in the field by adding a half-saturated (at 20°C) solution of $HgCl_2$ (150 µL) through the rubber seal of each bottle using a syringe, as described above the 72 incubation bottles, resulting in a concentration of 161 µM similar to previous studies (Clayer et al., 2021; Hessen et al., 2017; Yang et al., 2015). Samples for DIC analysis were filled without bubbles in 100 ml Winkler glass bottles that were sealed airtight directly after sampling. These samples were not fixed in any way and were analysed by a TOC analyzer within two hours. Note that estimation of dissolved CO_2 concentrations from pH and DIC is the least uncertain method of indirect CO_2 concentration with estimated relative error of 6% or less (Golub et al., 2017). Lake water temperature and pH were measured *in-situ* using HOBO pH data loggers placed at 1, 1.5, 2 and 2.5 m (Elit, Gjerdrum, Norway).

Lake Lundebyvannet has a surface area of 0.4 km^2 and a maximum depth of 5.5 m. It often experiences large blooms of G. semen over the summer between May and September (Hagman et al., 2015; Rohrlack, 2020). The lake water is characterised by high and fluctuating concentrations of humic substances (with DOC concentrations ranging from 8 to 28 mg C L^{-1}), ammonium (5 to 100 µg

N L^{-1}), nitrate (20 to 700 µg N L^{-1}), total N (average of 612 µg N L^{-1}), phosphate (2 to 4 µg P L^{-1}), total P (average of 28 µg P L^{-1}; Rohrlack et al., 2020; Hagman et al., 2015), a fluctuating pH (from 5.5 to 7.3), weak ionic strength with alkalinity ranging between 30 and 150 µmol L^{-1}, and electric conductivity varying from 40 to 70 µS cm^{-1}. For more details, see Rohrlack *et al.* (2020).

Lake Lundebyvannet was selected for this experiment because it is representative of productive, low-ionic strength Northern Hemisphere lakes typically found in the southern part of granitic bedrock regions in North-East America and Scandinavia.

2.3. Analytical chemistry

Gas chromatography

Headspace was prepared by gently backfilling sample bottles with 20–30 mL helium (He; 99,9999%) into the closed bottle while removing a corresponding volume of water. Care was taken to control the headspace pressure within 5% of ambient and a slight He overpressure was released before equilibration. The bottles were shaken horizontally at 150 rpm for 1 h to equilibrate gases between sample and headspace. The temperature during shaking was recorded by a data logger. Immediately after shaking, the bottles were placed in an autosampler (GC-Pal, CTC, Switzerland) coupled to a gas chromatograph (GC) with He back-flushing (Model 7890A, Agilent, Santa Clara, CA, US). Headspace gas was sampled (approx. 2 mL) by a hypodermic needle connected to a peristaltic pump (Gilson Minipuls 3), which connected the autosampler with the 250 µL heated sampling loop of the GC.

The GC was equipped with a 20-m wide-bore (0.53 mm) Poraplot Q column for separation of CH_4, CO_2 and N_2O and a 60 m wide-bore Molsieve 5Å PLOT column for separation of O_2 and N_2, both operated at 38°C and with He as carrier gas. N_2O and CH_4 were measured with an electron capture detector run at 375°C with Ar/CH_4 (80/20) as makeup gas, and a flame ionization detector, respectively. CO_2, O_2, and N_2 were measured with a thermal conductivity detector (TCD). Certified standards of CO_2, N_2O, and CH_4 in He were used for calibration (AGA, Germany), whereas air was used for calibrating O_2 and N_2. The analytical error for all gases was lower than 2%. For the Lake Lundebyvannet time series, CO_2 was separated from other gases using the 20 m wide-bore (0.53 mm) Poraplot Q column while the other gases were not measured.

The results from gas chromatography give the relative concentration of dissolved gases (in ppm) in the headspace in equilibrium with the water. For the lab experiment with Svartkulp samples (section 2.1), the concentration of dissolved gases in the water at equilibrium with the headspace were calculated from the temperature corrected Henry constant in water using Carroll, Slupsky and Mather (1991) for CO_2, Weiss and Price (1980) for N_2O, Yamamoto, Alcauskas and Crozier (1976) for CH_4, Millero, Huang and Laferiere (2002) for O_2, Hamme and Emerson (2004) for N_2. For the Lake

Lundebyvannet time series (section 2.2), the concentration of CO_2 in the water samples were determined using temperature-dependent Henry's law constants given by Wilhelm, Battino and Wilcock (1977). The quantities of gases in the headspace and water were summed to find the concentrations and partial pressures of dissolved gases from the water collected in the field as follows:

$$[gas] = \frac{p_{gas}HV_{water} + \frac{p_{gas}V_{headspace}}{RT}}{V_{water}} \qquad \text{(Eq. 1)}$$

where [gas] is the gas aqueous concentration, p_{gas} is the gas partial pressure, H is the Henry constant, V_{water} is the volume of water sample during headspace equilibration, $V_{headspace}$ is the headspace gas volume during equilibration, R is the gas constant and T the temperature during headspace equilibration (recorded during shaking). The calculations were similar to Yang *et al.* (2015).

DIC analyses

DIC analysis was performed for the Lake Lundebyvannet time series using a Shimadzu TOC-V CPN (Oslo, Norway) instrument equipped with a non-dispersive infrared (NDIR) detector with O_2 as a carrier gas at a flow rate of 100 mL min^{-1}. Two to three replicate measurements were run per sample. The system was calibrated using a freshly prepared solution containing different concentrations of $NaHCO_3$ and Na_2CO_3 and standards were measured in between each 6th sample. CO_2 concentrations in water samples ($[CO_2]$) were calculated on the bases of temperature, pH and DIC concentrations as follows (Rohrlack *et al.*, 2020):

$$[CO_2] = \frac{[H^+]^2 C_T}{Z} \qquad \text{(Eq. 2)}$$

where $[H^+]$ is the proton concentration (10^{-pH}), C_T is the dissolved inorganic carbon concentration and Z is given by:

$$Z = [H^+]^2 + K_1[H^+] + K_1K_2 \qquad \text{(Eq. 3)}$$

where K_1 and K_2 are the first and second carbonic acid dissociation constant adjusted for temperature (pK_1 = 6.41 and pK_2 = 10.33 at 25°C; Stumm & Morgan, 1996).

2.4. Data analysis

pCO_2 and saturation deficit

Lake Lundebyvannet CO_2 concentrations provided by GC and DIC analyses were converted to pCO_2 (in µatm) as follows:

$$pCO_2 = \frac{[CO_2]}{0.987 \times K_H \, P_{atm}} \quad \text{(Eq. 4)}$$

where K_H is Henry constant for CO_2 adjusted for in-situ water temperature (Stumm & Morgan, 1996) and P_{atm} is the atmospheric pressure in bar approximated by:

$$P_{atm} = (1013 - 0.1 \times altitude) \times 0.001 \quad \text{(Eq. 5)}$$

where $altitude$ is the altitude above sea level of Lake Lundebyvannet (158 m). Finally, the CO_2 saturation deficit (Sat_{CO_2} in µatm) was given by

$$Sat_{CO_2} = pCO_2 - [CO_2]_{air} \quad \text{(Eq. 6)}$$

where $[CO_2]_{air}$ is the pCO_2 in the air (416 µatm for 2020 in Southern Norway retrieved from EBAS database; NILU, 2022; Tørseth et al., 2012). Sat_{CO_2} gives the direction of CO_2 flux at the water-atmopshere interface, and its product with gas transfer velocity determine the CO_2 flux at the water-atmosphere interface, i.e., whether lake ecosystems are sink ($Sat_{CO_2} < 0$) or source ($Sat_{CO_2} > 0$) of atmospheric CO_2.

Statistical analyses

The effect of storage time and treatment on five dissolved gases (O_2, N_2, CO_2, CH_4, N_2O) from the Lake Svartkulp samples was tested with a two-way ANOVA at an alpha level adapted using the Bonferroni correction for multiple testing, i.e., α=0.05/5=0.01. To evaluate the impact of Hg fixation on Lake Lundebyvannet samples, $[CO_2]$ values determined by headspace equilibration and GC analysis of $HgCl_2$-fixed samples were compared with those calculated from DIC measurements of unfixed samples with a paired t-test.

A regression analysis was performed to describe the overestimation of CO_2 concentrations caused by $HgCl_2$ fixation in Lake Lundebyvannet samples as a function of pH. The total CO_2 concentration in the $HgCl_2$-fixed samples ($[CO_2]_{HgCl_2}$) can be expressed as:

$$[CO_2]_{HgCl_2} = [CO_2]_i + [CO_2]_{ex} \quad \text{(Eq. 7)}$$

where $[CO_2]_i$ is the initial CO_2 concentration prior to $HgCl_2$ fixation, i.e., CO_2 concentration in the unfixed samples, and $[CO_2]_{ex}$ is the excess CO_2 concentration caused by a decrease in pH following $HgCl_2$ fixation. The relative CO_2 overestimation (E in %) is given by:

$$E = \frac{[CO_2]_{HgCl_2} - [CO_2]_i}{[CO_2]_i} = \frac{[CO_2]_{ex}}{[CO_2]_i} \quad \text{(Eq. 8)}$$

The impact of pH (or $[H^+]$) on E was mathematically described by running a regression analysis using MATLAB®. The *fminsearch* MATLAB function from the Optimization toolbox was used to find the minimum sum of squared residuals (SSR) for functions of the form of: $E = A/[H^+]$ or $E = A \times 10^{-B \times pH}$. For each optimal solution, the root-mean-square error (RMSE) and coefficient of determination (R^2) were calculated against observed values of E, i.e., values of E determined empirically from observed $[CO_2]_i$ and $[CO_2]_{ex}$.

Chemical speciation, saturation-index calculations, and prediction of CO_2 overestimation

The speciation of solutes and saturation index values (SI) of selected minerals were calculated with the program PHREEQC developed by the USGS (Parkhurst & Appelo, 2013), neglecting the effect of dissolved organic matter. This was used to assess the impact of the addition of preservative on pH and shifting the carbonate equilibrium as well as dissolved inorganic carbon losses due to carbonate mineral precipitation. PHREEQC is commonly used to calculate the speciation of inorganic carbon, the SI of carbonate minerals and to help estimate the fate of inorganic carbon in carbon cycling studies (Atekwana et al. 2016; Clayer et al. 2016; Klaus 2023). For each PHREEQC simulation, two files, respectively the database (with input reactions) and input files, were used to define the thermodynamic model and the type of calculations to perform. The database of MINTEQA2 (e.g., *minteq.dat*, Allison et al., 1991) was used to describe the chemical system because it includes, inter alia, reactions and constants for Ag, Cu and Hg complexation with Cl, NO_3 and carbonates.

Three PHREEQC simulations were run representing the addition of each preservative solution to sample water from Lake Svartkulp. The input files described the composition of two aqueous solutions: (i) the preservative solution assumed to contain only the preservative (i.e., $HgCl_2$ solution) and (ii) sample water from Lake Svartkulp with observed major element concentrations (pH, Al, Ca, Cl, Cu, Fe, Mg, Mn, N as nitrate, K, Na, S as sulfate, Zn; Tab. S1) and Hg and Ag natural concentration assumed to be 10^{-5} mg/L. The output file provided the activities of the various solutes in the preserved samples, i.e., simulating the mixing of 120 mL of lake water with 240 µL of the $AgNO_3$, $CuCl_2$ and $HgCl_2$ preservative solutions, as described in section 2.1. This procedure allows to estimate the pH of the preserved samples as well as SI for various mineral phases. The SI is calculated by PHREEQC comparing the chemical activities of the dissolved ions of a mineral (ion activity product, IAP) with their solubility product (Ks). When SI > 1, precipitation is thermodynamically favourable. Note however that PHREEQC does not give information about precipitation kinetics.

Similarly, PHREEQC was used to estimate the decrease in pH caused by adding 150 µL of a half-saturated $HgCl_2$ solution to Lake Lundebyvannet samples prior to GC analyses, as described in section 2.2. In absence of data on the chemical composition of Lake Lundebyvannet, we assumed that

it had the same composition as Lake Svartkulp water samples. This assumption is supported by the fact that waters from both lakes have circumneutral pH, low ionic strength (poor buffering capacity) and high DOC concentration and would therefore behave similarly in presence of acids. Briefly, for each 0.1 pH value between pH of 5.4 and 7.3, the carbonate alkalinity was first adjusted by increasing HCO_3 concentrations in the input files for PHREEQC to confirm that the water was at equilibrium at the given pH value. Then, the effect of adding 150µL of a half-saturated $HgCl_2$ solution was simulated as described above for Lake Svartkulp. Knowing the new equilibrated pH, after addition of $HgCl_2$, the overestimation of CO_2 concentration in Hg-fixed samples relative to unfixed samples (E, described in Eq. 8 above) can be predicted as described below.

Adapting Eq. (2), we obtain:

$$[CO_2]_{HgCl_2} = \frac{[H^+]^2_{HgCl_2}\, C_T}{Z_{HgCl_2}} \qquad \text{(Eq. 9)}$$

and

$$[CO_2]_i = \frac{[H^+]_i^2 C_T}{Z_i} \qquad \text{(Eq. 10)}$$

where $[H^+]_i$ is the proton concentration measured in the initial water samples prior to $HgCl_2$ fixation, and $[H^+]_{HgCl_2}$ is the proton concentration estimated by PHREEQC following $HgCl_2$ fixation, and similarly for Z_i and Z_{HgCl_2} from Eq. (3). Combining Eqs. (7), (9) and (10) we obtain:

$$[CO_2]_{ex} = C_T \left(\frac{[H^+]^2_{HgCl_2}}{Z_{HgCl_2}} - \frac{[H^+]_i^2}{Z_i} \right) \qquad \text{(Eq. 11)}$$

Hence:

$$E = \frac{[CO_2]_{ex}}{[CO_2]_i} = \frac{\left(\frac{[H^+]^2_{HgCl_2}}{Z_{HgCl_2}} - \frac{[H^+]_i^2}{Z_i} \right)}{\frac{[H^+]_i^2}{Z_i}} \qquad \text{(Eq. 12)}$$

Alternatively, E can also simply be predicted based on the carbonic acid dissociation:

$$CO_2 + H_2O \overset{K_1}{\Leftrightarrow} HCO_3^- + H^+ \qquad \text{(Reaction 1)}$$

At equilibrium, we have:

$$K_1 = \frac{[HCO_3^-][H^+]}{[CO_2]} \qquad \text{(Eq. 13)}$$

When pH is decreased upon addition of $HgCl_2$, a fraction (α) of the initial bicarbonate concentration $[HCO_3^-]_i$ is turned into CO_2. This fraction, expressed as $[CO_2]_{ex}$ in Eq. (7) above, can be estimated with Eq. 13 as follows:

$$[CO_2]_{ex} = \alpha[HCO_3^-]_i = \frac{\alpha K_1 [CO_2]_i}{[H^+]_i} \qquad \text{(Eq. 14)}$$

Introducing the expression of $[CO_2]_{ex}$ from Eq. 14 into Eq. 8 yields:

$$\frac{[CO_2]_{ex}}{[CO_2]_i} = E = \frac{\alpha K_1}{[H^+]_i} \qquad \text{(Eq. 15)}$$

When the decrease in pH, or acidification, is greater than the buffering capacity of the water: $\alpha = 1$. The value of α cannot exceed 1 because the amount of CO_2 produced by a decrease in pH cannot exceed the amount of HCO_3^- initially present. In all the other cases, we have: $\alpha < 1$. For both predictions of E, i.e., with Eqs. 12 and 15, the root-mean-square error (RMSE) and coefficient of determination (R^2) were calculated.

Finally, additional sources of CO_2 overestimation were investigated by analysing the residuals of the model described by Eq. 12, i.e., the difference between E predicted with Eq. 12 and E determined empirically with Eq. 8. Briefly, residuals were plotted against pH and *in situ* temperature. Residuals were separated in two groups based on the empirical value of $[HCO_3^-]_i - [CO_2]_{ex}$, i.e., the first group had values of $[HCO_3^-]_i - [CO_2]_{ex} \geq a$ while the second group had values of $[HCO_3^-]_i - [CO_2]_{ex} \leq -a$ where different values for a were used: 20, 10 or 5 µM. The justification for separating residuals in two groups is that: (i) the first group represents samples for which bicarbonate alkalinity in the original sample is, as expected, higher than CO_2 overestimation after $HgCl_2$-fixation, while (ii) the second group represents samples for which bicarbonate alkalinity is not sufficient to explain CO_2 overestimation after $HgCl_2$-fixation.

CO_2 diffusion fluxes from Lake Lundebyvannet

The diffusive flux of CO_2 (F_{CO_2} in mol m^{-2} d^{-1}) from Lake Lundebyvannet surface water was estimated according to:

$$F_{CO_2} = \frac{k_{CO_2}([CO_2] - [CO_2]_{eq})}{1000} \qquad \text{(Eq. 16)}$$

where k_{CO_2} is the CO_2 transfer velocity in m d^{-1}, $[CO_2]$ is the surface water CO_2 concentration (µM), and 1000 is a factor to ensure consistency in the units and $[CO_2]_{eq}$ is the theoretical water CO_2 concentration (µM) in equilibrium with atmospheric CO_2 concentration calculated with Eq. (3) and pCO_2 of 416 µatm (see above).

The CO_2 transfer velocity (k_{CO_2}) was estimated as follows (Vachon & Prairie, 2013):

$$k_{CO_2} = k_{600}\left(\frac{600}{Sc_{CO_2}}\right)^{-n} \qquad \text{(Eq. 17)}$$

where k_{600} is the gas transfer velocity (m d^{-1}) estimated from empirical wind-based models and Sc_{CO_2} is the CO_2 Schmidt number for in situ water temperature (unitless; Wanninkhof, 2014). We used n values of 0.5 or 2/3 when wind speed was below or above 3.7 m s^{-1}, respectively (Guérin et al., 2007). Empirical k_{600} models included those from Cole & Caraco (1998; $k_{600} = 2.07 + 0.215U_{10}^{1.7}$), Vachon & Prairie (2013; $k_{600} = 2.51 + 1.48U_{10} + 0.39U_{10}\log_{10} LA$) and Crusius & Wanninkhof (2003; power model: $k_{600} = 0.228U_{10}^{2.2} + 0.168$ in cm h^{-1}). U_{10} and LA refer to mean wind speed at 10 m in m s^{-1} and lake area in km^2, respectively. Sub-hourly U_{10} data for 2020 was retrieved from a weather station of the Norwegian Meteorological Institute located 1.5 km west of Lake Lundebyvannet (station name: E18 Melleby; ID: SN 3480; 59.546 N, 11.4535E) using the Frost application programming interface (*Frost API*, 2022). Daily, monthly, and yearly (only covering the ice-free season: April-November) F_{CO_2} was estimated using Eq. (12). Daily [CO_2] was interpolated from weekly data using a modified Akima spline (makima spline in Matlab® based on Akima, 1974). This interpolation method is known to avoid excessive local undulations.

3. Results

3.1. Effects of preservatives and storage time on dissolved gases

In the unfixed samples from Lake Svartkulp, the concentration of O_2 declined while CO_2 increased over time in a close to 1:1 molar ratio, likely reflecting the effect of microbial respiration activity and mineralisation of organic matter (Fig. 2, Tab. S2). Concentration of O_2 in the unfixed samples decreased from near 300 to below 200 µM (Fig. 2). In the presence of inhibitors, O_2 concentrations tended to be slightly higher at t=24h and remained constant or declined only slightly over time to generally remain at or above saturation (280 to 300 µM). Thus, the inhibitors were effective in reducing oxic respiration.

The concentration of CO_2 in the presence of $AgNO_3$ at t = 24h was not significantly different to the unfixed at t = 0 (Fig 2; paired t-test, P>0.1). At t = 24h, CO_2 concentrations were however much higher in the presence of $HgCl_2$ (135 µM) or $CuCl_2$ (131 µM) than in the unfixed (89 µM; Fig 2, Tab. S2). The CO_2 further increases from 130 µM to ~160 µM after 3 weeks in both sample sets preserved with $HgCl_2$ and $CuCl_2$ while a decrease in O_2 is less pronounced for samples fixed with $CuCl_2$ and completely absent for samples fixed with $HgCl_2$. Overall, the addition of $HgCl_2$ or $CuCl_2$ following sampling increased CO_2 concentrations by 47% after 24h compared to the unfixed and caused further changes over the three-month storage time, while preservation with $AgNO_3$ yielded CO_2

concentrations consistent with the unfixed and caused negligible changes over time (Fig. 2; paired t-test, P>0.1).

The concentration of CH_4 across all samples ranged between 0.017 and 0.377 µM (Fig. 2), as expected two orders of magnitude smaller than CO_2. At t = 24h, the concentration of CH_4 was over 0.2 µM in the presence of inhibitors while it was below saturation in the unfixed (0.03 µM; Fig. 2). CH_4 oversaturation in the preserved samples persisted after three weeks and three months of storage and CH_4 concentration remained unchanged (Fig. 2, Tab. S2).

The concentration of N_2O ranged between 9.8 and 12.7 nM with only samples preserved with $AgNO_3$ showing negligible changes over time (Fig. 2; paired t-test, P>0.1). All the other samples showed consistent patterns with storage time. N_2O concentrations initially increased within the first 3 weeks, followed by a decrease after 3 months.

The changes in N_2 were likely within handling and analytical errors and not different in the presence or absence of inhibitors (Fig. 2; Tab. S2; paired t-test, P>0.1).

3.2. Effects of preservatives on pH

In the samples amended with ultrapure water or $AgNO_3$, the pH did not show any significant changes after 2h or 24h. In contrast, both groups with $HgCl_2$ and $CuCl_2$ treatments show significant decreases of pH after 2h, -0.12 and -0.19, respectively, and 24h, -0.16 and -0.21, respectively. In addition, they showed a significant decrease in pH from 2h to 24h. Samples amended with $CuCl_2$ show the strongest decrease in pH.

3.3. Contrasting impacts of $HgCl_2$, $CuCl_2$ and $AgNO_3$ on dissolved CO_2 estimation revealed by chemical speciation modelling

The PHREEQC simulation of unpreserved samples, based on concentrations of all major elements (Tab. S1), predicted a pH of 6.72 (Tab. 2) which is very close to the measured pH of 6.73 (Tab. S1). This suggests that chemical information provided to PHREEQC is likely sufficient to describe the system, without having to invoke more complex reactions with dissolved organic matter. The addition of $HgCl_2$ and $CuCl_2$ both caused a significant decrease in pH to 6.40 and 6.45, respectively (Tab. 2) which is similar to the decrease observed at the end of the 24h short term incubation (Fig. 2).

In absence of preservatives, none of the common carbonate minerals, including calcite, were associated with a saturation index higher than 1, i.e., dissolution was thermodynamically favourable for all these minerals and no DIC loss was expected (Tab. 2). However, upon addition of $HgCl_2$ or $CuCl_2$, some carbonate minerals, e.g., $HgCO_3$ or malachite and azurite, respectively, were expected to spontaneously precipitate given their relatively high saturation index values.

456 3.3. Effects of $HgCl_2$ on dissolved CO_2 concentration under a range of pH

457 CO_2 concentrations in unfixed water samples from Lake Lundebyvannet were significantly lower than
458 in the $HgCl_2$-fixed samples (mean difference: 52 µM; paired t-test; $P<0.0001$; Tab. 3). Fixation with
459 $HgCl_2$ caused a general overestimation of CO_2 concentration and the saturation deficit (Fig. 4), thus
460 missing out events of CO_2 influx (carbon sink) under high photosynthesis activity (high pH; Fig. 4).
461 In parallel, PHREEQC predicted a decrease of 0.6 to 1.8 units of pH related to $HgCl_2$ addition (Fig.
462 S1).

463 The pH value of water samples from Lake Lundebyvannet varied between 5.4 and 7.3 (Fig 4 and 5),
464 mainly due to marked variations in phytoplankton photosynthetic activity (Rohrlack et al., 2020). The
465 relative overestimation of CO_2 (E) follows an exponential increase with pH and is well reproduced by
466 a simple exponential function ($2.56 \times 10^{-5} \times 10^{1.015 \times pH}$,RMSE=44%, R^2=0.81, $p<0.0001$; Fig. 5).

467

468 **4. Discussion**

469 Prior to using dissolved gas concentrations in freshwater to estimate the magnitude of biological
470 aquatic processes such as photosynthesis and oxic respiration, denitrification and methanogenesis, we
471 must ensure that biological activity between sampling and laboratory analyses was efficiently
472 inhibited without significant impacts on the sample's chemistry. Here we report a unique dataset on
473 the impact of three preservatives on water samples from a typical low-ionic strength, unproductive
474 boreal lake to inform on potential risks of mis-estimation of dissolved gas concentrations. We further
475 show, using CO_2 concentration data from a typical productive boreal lake, that using $HgCl_2$ can lead
476 to negligence of the role of photosynthesis in lake C cycling.

477 4.1 Best preservative for the determination of dissolved gas concentrations

478 Given that none of the four treatments (unfixed, $HgCl_2$, $CuCl_2$ or $AgNO_3$) applied to Lake Svartkulp
479 water samples during the 3-month incubation offer an independent control, a first challenge is to
480 determine which of the treatment represent the most realistic dissolved gas concentrations close to
481 real condition. For CO_2 and O_2, a few studies have used unfixed samples (only preserved dark at
482 +4°C) up to 48h after sampling to determine CO_2 or DIC concentrations (e.g., Sobek et al. 2003,
483 Kokic et al., 2015). So, the CO_2 and O_2 concentrations in the unfixed samples collected after 24h
484 incubation are the most representative of the initial real concentrations. Biological activity might have
485 had an impact, but this is likely negligible over the first 24h. In addition, the fact that the CO_2 and O_2
486 concentrations in the samples fixed with $AgNO_3$ after 24h, three weeks and three months are equal to
487 those from unfixed samples after 24h (Fig. 2) confirms that the unfixed samples after 24h can be used
488 as a control. In fact, only samples fixed with $AgNO_3$ are trustful given the expected toxicity of Ag, the
489 absence of impact on pH (Fig. 3), and unchanged concentrations over the three-month experiment for

all gases. Similarly, N_2O and N_2 concentrations in the unfixed samples after 24h can be used as control. However, for CH_4, Fig. 2 shows that already after 24h, the CH_4 concentration in the unfixed samples is below atmospheric saturation while it is consistently much higher in all three sets of fixed samples. Boreal lakes are typically over saturated with respect to CH_4 (Valiente et al., 2022) and it is very unlikely that CH_4 could have been produced in lake water incubated under high concentration of oxygen and toxic preservatives. Hence, unfixed samples do not represent real CH_4 concentrations. These observations are all consistent with the fact that the three preservatives were effective in preserving CH_4 from oxidation. Even over 24h, preservatives need to be added to oxic water samples to preserve CH_4 from oxidation. In fact, oxic methanotrophy typically show rates in the order of µM day^{-1} (Thottathil et al., 2019; van Grinsven et al., 2021). Hence, a CH_4 consumption of 0.3 µM within 24h in the unfixed water samples is realistic (Fig. 2).

In summary, preservation with $AgNO_3$ is the only method that offered robust determination of all five dissolved gases with negligible changes in concentration over time.

4.2 Risks of mis-estimating dissolved gas concentration with $HgCl_2$ and $CuCl_2$ preservation

Both sets of samples preserved with either $HgCl_2$ and $CuCl_2$ showed CO_2 concentrations that were much higher than the unfixed (after 24h) or the $AgNO_3$-fixed samples. This is due to an acidification of the poorly buffered (alkalinity 127 µM) and near neutral water (pH=6.73), shifting the carbonate equilibrium from HCO_3 to CO_2 as also shown by Borges et al. (2019). In fact, a rapid decrease in pH was observed upon $HgCl_2$ and $CuCl_2$ treatments (Fig. 3). The increase of CO_2 from about 130 µM to ~160 µM after 3 weeks in both sample sets preserved with $HgCl_2$ and $CuCl_2$ is not mirrored by a similar decrease in O_2 (Fig. 2). This suggests that oxic respiration is not the main source for this additional 30 µM of CO_2 but rather points towards additional acidification of the samples caused, e.g., by kinetically controlled complexation of Hg^{2+} with dissolved organic matter (Miller et al., 2009). In fact, the relatively slow complexation of Hg^{2+} with organic thiol groups can release two protons (Skyllberg, 2008) and up to three, with some participation of a third weak-acid group (Khwaja et al., 2006). The transient nature of acidification caused by $HgCl_2$ and $CuCl_2$ is also evident in the pH impacts showing higher acidification after 24h than after 2h incubation (Fig. 3). The following decrease in CO_2 after 3 months (down to ~145 µM) points to other processes. The precipitation of Hg and Cu carbonates, given their high saturation index values (Tab. 2), would be consistent with the decrease in CO_2 concentrations observed between three weeks and three months. Calcite precipitation is typically observed in supersaturated solutions within 48h (Kim et al., 2020). Hence, it is realistic to consider that Hg and Cu carbonate precipitation influenced the CO_2 concentration within the preserved samples over the three months of storage time. Impacts of Hg or Cu carbonate precipitation is not evident after three weeks likely because of slow but persistent CO_2 production in presence of

524 $HgCl_2$ and $CuCl_2$ related to acidification as described above (Fig. 2). However, after three weeks, this
525 production likely weakens and is counterbalanced by increasing carbonate precipitation.

526 Overall, the addition of $HgCl_2$ or $CuCl_2$ following sampling increased CO_2 concentrations by 47%
527 within the first 24h compared to the unfixed consistent with the -0.16 to -0.21 pH-unit acidification
528 observed over the same time in the pH incubation experiment (Fig. 3) and the pH estimated with
529 PHREEQC without the interaction with dissolved organic matter (Tab. 2). In fact, introducing pH and
530 CO_2 concentration values of 6.40–6.45 and 130 µM, respectively, for the samples preserved with
531 $HgCl_2$ and $CuCl_2$ into Eqs. 1 and 2 yields DIC concentrations (C_T) of about 270 µM at t=24h. These
532 DIC concentrations are almost equal to those calculated for the unfixed samples and those preserved
533 with $AgNO_3$ at t = 24h, i.e., with a pH of 6.73 and CO_2 concentration of 88 µM. Interestingly, the
534 concentration of CO_2 in the samples preserved with $HgCl_2$ and $CuCl_2$ continues to increase up to ~160
535 µM after 3 weeks. Given that oxic respiration is inhibited (Fig. 2), this additional CO_2 is believed to
536 originate from progressive release of protons following relatively slow complexation of Hg^{2+} with
537 dissolved organic matter (Khwaja et al., 2006; Miller et al., 2009; Skyllberg, 2008). Note however
538 that this process could not be predicted with PHREEQC given that it neglected the effect of dissolved
539 organic matter.

540 Unlike the $AgNO_3$-fixed samples, all the other samples showed an initial increase in N_2O
541 concentration from 24h to 3 weeks, followed by a decrease from three weeks to 3 months. Similar
542 patterns of net N_2O production followed by net consumption were also reported in short-term
543 incubations of seawater from the high latitude Atlantic Ocean, although over much shorter timescales,
544 i.e., 48 and 96h (Rees et al., 2021). The large difference in kinetics between the latter experiment
545 (Rees et al., 2021) and our incubation might be attributable to differences in incubation temperature
546 where the seawater from the high latitude Atlantic Ocean was incubated at ambient temperatures
547 while our samples were kept at +4°C. Other difference in the experimental setup might have also
548 played a role. The lack of inhibition of N_2O production and consumption in the samples preserved
549 with $HgCl_2$ and $CuCl_2$ can be attributed to the fact that N_2O production tends to increase under
550 increasing acidic conditions (Knowles, 1982; Mørkved et al., 2007; Seitzinger, 1988). In fact, the
551 mole fraction of N_2O produced during denitrification increases compared to N_2 as pH decreases
552 (Knowles, 1982).

553

554 4.3 Using PHREEQC to estimate acidification caused by $HgCl_2$ in samples from Lake Lundebyvannet

555 As for the samples from Lake Svartkulp as described above, the overestimation of CO_2 concentration
556 in the samples from Lake Lundebyvannet fixed with $HgCl_2$ (161 µM added; Fig. 4) likely stems from
557 the acidification shifting the carbonate equilibrium from bicarbonate to CO_2. In fact, PHREEQC
558 predicted a decrease of 0.6 to 1.8 units of pH related to $HgCl_2$ addition in these samples (Fig. S1).

559 The relative overestimation of CO_2 (*E* in Fig. 5) followed a typical exponential increase reflecting the
560 decrease in absolute CO_2 concentration with increasing pH (Stumm & Morgan, 1981) caused here by
561 phytoplankton photosynthesis. In fact, the exponential increase in CO_2 overestimation is easily
562 predicted by Eq. (9) with an equivalent level of accuracy as the optimized exponential function (Fig.
563 5). Consistently, the relative overestimation of CO_2 (*E*) shows an inverse decrease with $[H^+]$ that is
564 well reproduced by a simple inverse function ($3.25 \times 10^{-5}/[H^+]$; RMSE=44%, R^2=0.81, p<0.0001;
565 Fig. 5) and predicted by Eq. (15), with an α value of 1. Combining Eqs. 8 and 15 and solving it with
566 pH values estimated from PHREEQC (Fig. S1) for α yields values ranging between 0.72 and 0.89
567 with an average of 0.85. Unexpectedly, this average α value is almost equal to the ratio of the inverse
568 function coefficient and K_1, i.e., $\frac{3.25\times10^{-5}}{K_1} = 0.87$. Hence, the relative overestimation of CO_2 (*E*)
569 caused by $HgCl_2$ fixation is easily predicted by the change in bicarbonate equilibrium knowing the
570 proton release from $HgCl_2$ addition, here estimated with PHREEQC.

571 Hence, PHREEQC can be used to predict decrease in pH caused by $HgCl_2$ fixation, if sufficient
572 knowledge is gathered on the ionic water composition. Proton release during $HgCl_2$ fixation can be
573 represented by the following reaction:

574 $$HgCl_2 + 2H_2O = Hg(OH)_2 + 2H^+ + 2Cl^- \qquad \text{(Reaction 2)}$$

575 From reaction 2, it becomes evident that the initial concentration of chloride in the water samples will
576 likely limit $HgCl_2$ dissociation and proton release. This is a likely mechanism occurring in seawater
577 where $HgCl_2$ has been shown to cause a decrease in pH, although at a negligible level with a
578 maximum decrease in pH of -0.01 (Chou et al., 2016).

579 Figure 3 shows that a range of water samples were associated with a relative CO_2 overestimation (*E*)
580 that substantially deviated from the overestimation predicted with Eq. 12 (red and blue symbols in
581 Fig. 5). In fact, some samples had a higher initial bicarbonate content ($[HCO_3^-]_i$) than the excess CO_2
582 concentration ($[CO_2]_{ex}$), while other showed the opposite. The former case (blue symbols in Fig. 5)
583 can easily be explained by a higher buffering capacity of the sampled water, i.e., a higher pH after
584 $HgCl_2$-fixation than that predicted by PHREEQC related to a different water composition. Indeed, the
585 concentration of major elements in the water from Lake Lundebyvannet may vary significantly over
586 time, and in absence of data, we considered that the water composition, except for DIC, pH and
587 $HgCl_2$, was constant over time. By contrast, samples associated with $[CO_2]_{ex}$ being larger than
588 $[HCO_3^-]_i$ are more enigmatic. In order to shed light on possible explanations, we visually inspected
589 trends between empirical deviations from predictions, i.e., residuals, and *in situ* temperature or pH.
590 Absolute values of residuals showed a progressive increase with pH and *in situ* temperature which is
591 in agreement with decreasing precision of the headspace method with increasing temperature and pH
592 (Koschorreck et al., 2021). In fact, CO_2 is less soluble at higher temperature, hence more gas can

evade during sampling, and thus the error increases with *in situ* temperature. In addition, at higher pH, CO_2 concentration decreases and consequently the absolute error on CO_2 quantification becomes larger relative to measured CO_2 concentration. Interestingly, many of the high residual values were not evenly distributed across the year, nor across the summer and were rather associated with only a few specific sampling events during summer (Fig. S2). This suggests that degassing could have occurred due to high ambient temperature in the field. Water associated with $[CO_2]_{ex}$ being larger than $[HCO_3^-]_i$ (red symbols in Fig. 5 and S4) could have been subject to a larger degassing in the samples collected for DIC analysis than the samples for GC analysis. On the other hand, degassing was likely larger for samples for GC analysis than for DIC analysis for water associated with $[HCO_3^-]_i$ being larger than $[CO_2]_{ex}$ (blue symbols in Fig. 5 and Fig. S2). In addition to degassing and temperature effects, errors in pH measurements can also cause a large misestimation of CO_2 concentration from DIC analysis, and this error increases exponentially with pH following the shift in carbonate equilibrium. In summary, our analysis is consistent with that of Koschorreck et al. (2021) showing that errors in the determination of CO_2 concentrations are smaller at lower pH and lower temperature (Fig. S2).

4.4. Implications for the estimation of lake and reservoir C cycling and recommendations

Using $HgCl_2$ or $CuCl_2$ to preserve dissolved gas samples in poorly buffered water samples has large impacts on CO_2 concentrations with considerable risk of leading to incorrect interpretations. The risk of mis-estimating CO_2 concentration due to $HgCl_2$ and $CuCl_2$ preservation is the highest when pH of the unfixed water is close to the first carbonic acid dissociation constant (pK_1 = 6.41 at 25°C; Stumm & Morgan, 1996). It implies that any small shift in pH will have a significant impact in the carbonate equilibrium between bicarbonate to CO_2. The risk is also the highest in the lowest ionic strength waters. In that respect, low-ionic strength, slightly acidic to neutral, moderately humic lakes commonly found in Norway (de Wit et al., 2023), large parts of Sweden (Valina et al. 2014), and Finland, Atlantic Canada (Houle et al., 2022), Ontario, Québec, and North-East USA (Skjelkvåle and de Wit 2011; Weyhenmeyer et al., 2019) are the most prone to errors in CO_2 concentrations related to $HgCl_2$ or $CuCl_2$ preservation. Through a preliminary literature search we found several studies from boreal lakes (Jonsson et al., 2001; Urabe et al., 2011; Yang et al., 2015; Hessen et al., 2017) but also from circum-neutral pH sub-tropical to tropical aquatic environments (Jeffrey et al., 2018; Webb et al., 2018; Ray et al., 2021) where preservation with $HgCl_2$ may have caused biases in the quantification of CO_2 concentrations as it was the case for samples from the Congo River (Borges et al., 2019). A significant part of the low-ionic strength boreal lakes become increasingly sensitive to changes in nutrients with strong impacts on their role in carbon cycling (Myrstener et al., 2022). In this context, it is crucial to avoid mis-estimation of CO_2 concentrations and thus avoid use of $HgCl_2$ or $CuCl_2$ to ensure a robust understanding of the role of autotrophic processes in lake C cycling. Below

we describe the implications for the lake C budget of Lundebyvannet as an example of a mis-estimation of the role of photosynthesis in a typical productive boreal lake.

In Lake Lundebyvannet, over the ice-free season, average CO_2 concentrations determined following $HgCl_2$-fixation and GC analysis were 82% higher than those obtained from DIC analyses (Tab. 3; Fig. 6 and S3). CO_2 concentrations obtained from $HgCl_2$-fixed samples created the illusion that Lake Lundebyvannet was a steady net source of CO_2 to the atmosphere over the ice-free season with large CO_2 saturation deficit (Fig. 4) while, in reality, the lake switched from being a net source in May, to a net sink over a few weeks in June, and returning to a net source in July (Fig. 6 and S3). Indeed, monthly CO_2 overestimation related to $HgCl_2$-fixation reached about 300% in June (Tab. 3). Propagating this overestimation into the estimates of CO_2 diffusion fluxes with typical wind-based models yields overestimation of CO_2 fluxes of 108–112% over the ice-free season and up to 2100% in June (Tab. 3 and S3). Hence, interpreting CO_2 data without correcting for CO_2 overestimation caused by $HgCl_2$-fixation leads to negligence of the role of photosynthesis in lake C cycling with major implications for current and future predictions of lake CO_2 emissions.

The use of $HgCl_2$ to preserve water samples prior to dissolved gas analyses is part of the current guidelines for greenhouse gas measurements in freshwater reservoirs (Machado Damazio et al., 2012; UNESCO/IHA, 2008, 2010). Hence, there is a risk of overestimating CO_2 concentrations and emissions, in absence of discrete measurement of emissions, from hydropower reservoirs with consequence on the present and expected greenhouse gas footprint from hydroelectricity. To ensure precise estimation of greenhouse gas concentration and, possibly, emission from hydropower, the use of $HgCl_2$ should therefore be discontinued.

5. Conclusion

Mercury is a potent neurotoxin for humans and toxic for the environment and its use should be discouraged, notably following the Minamata convention on mercury, a global treaty ratified by 126 countries (16 December 2020) to protect human health and the environment from the adverse effects of mercury. This study further questions the use of $HgCl_2$ for preservation of poorly buffered (low ionic strength) water samples with high DOC concentration for analysis of dissolved gases in the laboratory. Although $CuCl_2$ is less toxic, it behaved similarly to $HgCl_2$ and cannot be recommend. In fact, both chlorinated inhibitors caused a significant decrease in pH shifting the carbonate equilibrium towards CO_2 and are also suspected to promote carbonate precipitation over long-term storage. The only promising inhibitor tested in this study was $AgNO_3$ notably for dissolved CO_2, CH_4 and N_2O. Silver nitrate is a suitable substitute for $HgCl_2$ in low-ionic strength waters, further tests should be carried out with a range of inhibitor concentration and more diverse water samples. The use of chemical inhibitors may not be the best approach. Alternatives exist, such as directly measuring gas concentrations *in situ* with sensors, or sampling the headspace out in the field, and bringing back gas

samples (e.g., Cole et al., 1994; Karlsson et al., 2013; Kling et al., 1991; Valiente et al., 2022), rather than water samples, to the lab for gas chromatography analyses. However, care must be taken to know the exact equilibration temperature (Koschorreck et al., 2021) and to avoid gas exchange with the atmosphere as well as to use a clean background gas during headspace equilibration which can be challenging in remote environments under harsh meteorological conditions.

We further advise against interpretation of CO_2 concentration data from low ionic strength, circum-neutral water samples preserved with $HgCl_2$ or $CuCl_2$. The overestimation of CO_2 concentration caused by $HgCl_2$ can mask the effect of photosynthesis on lake carbon balance, creating the illusion that lakes are net CO_2 sources when they are net CO_2 sinks. Our analysis from Lake Lundebyvannet shows that $HgCl_2$ fixation led to an overestimation of the CO_2 concentration by a factor of 1.8, on average, but approaching a factor of 4 during the peak photosynthetic period. An even larger impact is expected on CO_2 diffusive fluxes which were overestimated by a factor of 2 on average and up to a factor of >20 during peak photosynthesis. Interpreting such data would have underestimated the current and future role of aquatic photosynthesis.

Data availability

All data supporting this study is available at https://doi.org/10.4211/hs.436be40748a246269102b20211b49762 (Clayer et al., 2024)

Author contribution

JET, AK, and TR supervised and PD, KN and FC contributed to the study design. JET, KN and TR carried out the experiments. PD and TR performed the chemical analyses. JET and FC wrote the first draft. FC performed the modelling, data, and statistical analyses, and drafted the figures. All co-authors edited the manuscript.

Competing interests

The contact author has declared that none of the authors has any competing interests.

Acknowledgements

We are grateful to Benoît Demars for research assistance, coordination, and useful comments and discussions on an earlier version of this manuscript and to Heleen de Wit for discussions. Research was funded by NIVA and through the Global Change at Northern Latitude (NoLa) project #200033.

References

693 Akima, H. (1974). A method of bivariate interpolation and smooth surface fitting based on local
694 procedures. *Communications of the ACM*, *17*(1), 18–20.
695 https://doi.org/10.1145/360767.360779
696 Allison, J., Brown, D., & Novo-Gradac, K. (1991). *MINTEQA2/PRODEFA2, a geochemical*
697 *assessment model for environmental systems: Version 3. 0 user's manual*. GA: US
698 Environmental Protection Agency.
699 Amorim, M. J. B., & Scott-Fordsmand, J. J. (2012). Toxicity of copper nanoparticles and CuCl2 salt
700 to Enchytraeus albidus worms: Survival, reproduction and avoidance responses.
701 *Environmental Pollution*, *164*, 164–168. https://doi.org/10.1016/j.envpol.2012.01.015
702 Atekwana, E. A., Molwalefhe, L., Kgaodi, O., & Cruse, A. M. (2016). Effect of evapotranspiration on
703 dissolved inorganic carbon and stable carbon isotopic evolution in rivers in semi-arid
704 climates: The Okavango Delta in North West Botswana. *Journal of Hydrology: Regional*
705 *Studies*, *7*, 1–13. https://doi.org/10.1016/j.ejrh.2016.05.003
706 Borges, A. V., Darchambeau, F., Lambert, T., Morana, C., Allen, G. H., Tambwe, E., Toengaho
707 Sembaito, A., Mambo, T., Nlandu Wabakhangazi, J., Descy, J.-P., Teodoru, C. R., &
708 Bouillon, S. (2019). Variations in dissolved greenhouse gases (CO_2, CH_4, N_2O) in the Congo
709 River network overwhelmingly driven by fluvial-wetland connectivity. *Biogeosciences*,
710 *16*(19), 3801–3834. https://doi.org/10.5194/bg-16-3801-2019
711 Carroll J.J., Slupsky J.D. & Mather A.E. (1991) The solubility of carbon dioxide in water at low
712 pressure. *Journal of Physical and Chemical Reference Data,* **20,** 1201-1209.
713 https://doi.org/10.1063/1.555900
714 Chen, C. Y., Driscoll, C., Eagles-Smith, C. A., Eckley, C. S., Gay, D. A., Hsu-Kim, H., Keane, S. E.,
715 Kirk, J. L., Mason, R. P., Obrist, D., Selin, H., Selin, N. E., & Thompson, M. R. (2018). A
716 Critical Time for Mercury Science to Inform Global Policy. *Environmental Science &*
717 *Technology*, *52*(17), 9556–9561. https://doi.org/10.1021/acs.est.8b02286
718 Chen H., Johnston R.C., Mann B.F., Chu R.K., Tolic N., Parks J.M. & Gu B. (2017) Identification of
719 mercury and dissolved organic matter complexes using ultrahigh resolution mass
720 spectrometry. *Environmental Science & Technology Letters,* **4,** 59-65.
721 https://doi.org/10.1021/acs.estlett.6b00460
722 Chou W.C., Gong G.C., Yang C.Y. & Chuang K.Y. (2016) A comparison between field and
723 laboratory pH measurements for seawater on the East China Sea shelf. *Limnology and*
724 *Oceanography-Methods,* **14,** 315-322. https://doi.org/10.1002/lom3.10091
725 Ciavatta L. & Grimaldi M. (1968) The hydrolysis of mercury(II) chloride, HgCl2. *Journal of*
726 *Inorganic and Nuclear Chemistry,* **30,** 563-581. https://doi.org/10.1016/0022-1902(68)80483-
727 X
728 Clayer, F., Gobeil, C., & Tessier, A. (2016). Rates and pathways of sedimentary organic matter
729 mineralization in two basins of a boreal lake: Emphasis on methanogenesis and
730 methanotrophy: Methane cycling in boreal lake sediments. *Limnology and Oceanography*,
731 *61*(S1), Article S1. https://doi.org/10.1002/lno.10323
732 Clayer, F., Thrane, J.-E., Brandt, U., Dörsch, P., & de Wit, H. A. (2021). Boreal Headwater
733 Catchment as Hot Spot of Carbon Processing From Headwater to Fjord. *Journal of*
734 *Geophysical Research: Biogeosciences*, *126*(12), e2021JG006359.
735 https://doi.org/10.1029/2021JG006359
736 Clayer, F., Thrane, J.-E., Dörsch, P., & Rohrlack T. (2024). Dataset for "Technical Note: Preventing
737 CO2 overestimation from mercuric or copper (II) chloride preservation of dissolved
738 greenhouse gases in freshwater samples"
739 https://doi.org/10.4211/hs.436be40748a246269102b20211b49762
740 Cole, J. J., Caraco, N. F., Kling, G. W., & Kratz, T. K. (1994). Carbon Dioxide Supersaturation in the
741 Surface Waters of Lakes. *Science*, *265*(5178), Article 5178.
742 https://doi.org/10.1126/science.265.5178.1568
743 Cole, J. J., & Caraco, N. F. (1998). Atmospheric exchange of carbon dioxide in a low-wind
744 oligotrophic lake measured by the addition of SF6. *Limnology and Oceanography*, *43*(4),
745 Article 4. https://doi.org/10.4319/lo.1998.43.4.0647
746 Crusius, J., & Wanninkhof, R. (2003). Gas transfer velocities measured at low wind speed over a lake.
747 *Limnology and Oceanography*, *48*(3), Article 3. https://doi.org/10.4319/lo.2003.48.3.1010

Deheyn, D. D., Bencheikh-Latmani, R., & Latz, M. I. (2004). Chemical speciation and toxicity of metals assessed by three bioluminescence-based assays using marine organisms. *Environmental Toxicology*, *19*(3), 161–178. https://doi.org/10.1002/tox.20009

de Wit, H. A., Garmo, Ø. A., Jackson-Blake, L. A., Clayer, F., Vogt, R. D., Austnes, K., Kaste, Ø., Gundersen, C. B., Guerrerro, J. L., & Hindar, A. (2023). Changing Water Chemistry in One Thousand Norwegian Lakes During Three Decades of Cleaner Air and Climate Change. Global Biogeochemical Cycles, 37(2), e2022GB007509. https://doi.org/10.1029/2022GB007509

Dickson A.G., Sabine C.L. & Christian J.R. (2007) *Guide to best practices for ocean CO2 measurements,* North Pacific Marine Science Organization.

Duan, Z., & Mao, S. (2006). A thermodynamic model for calculating methane solubility, density and gas phase composition of methane-bearing aqueous fluids from 273 to 523K and from 1 to 2000bar. *Geochimica et Cosmochimica Acta*, *70*(13), Article 13. https://doi.org/10.1016/j.gca.2006.03.018

Foti C., Giuffre O., Lando G. & Sammartano S. (2009) Interaction of inorganic mercury (II) with polyamines, polycarboxylates, and amino acids. *Journal of Chemical & Engineering Data,* **54,** 893-903. https://doi.org/10.1021/je800685c

Frost API. (2022). https://frost.met.no/index.html

Golub, M., Desai, A. R., McKinley, G. A., Remucal, C. K., & Stanley, E. H. (2017). Large Uncertainty in Estimating pCO2 From Carbonate Equilibria in Lakes. *Journal of Geophysical Research: Biogeosciences*, *122*(11), 2909–2924. https://doi.org/10.1002/2017JG003794

Guérin, F., Abril, G., Richard, S., Burban, B., Reynouard, C., Seyler, P., & Delmas, R. (2006). Methane and carbon dioxide emissions from tropical reservoirs: Significance of downstream rivers. *Geophysical Research Letters*, *33*(21). https://doi.org/10.1029/2006GL027929

Guérin, F., Abril, G., Serça, D., Delon, C., Richard, S., Delmas, R., Tremblay, A., & Varfalvy, L. (2007). Gas transfer velocities of CO2 and CH4 in a tropical reservoir and its river downstream. *Journal of Marine Systems*, *66*(1), Article 1. https://doi.org/10.1016/j.jmarsys.2006.03.019

Halmi, M. I. E., Kassim, A., & Shukor, M. Y. (2019). Assessment of heavy metal toxicity using a luminescent bacterial test based on Photobacterium sp. Strain MIE. *Rendiconti Lincei. Scienze Fisiche e Naturali*, *30*(3), 589–601. https://doi.org/10.1007/s12210-019-00809-5

Hagman, C. H. C., Ballot, A., Hjermann, D. Ø., Skjelbred, B., Brettum, P., & Ptacnik, R. (2015). The occurrence and spread of Gonyostomum semen (Ehr.) Diesing (Raphidophyceae) in Norwegian lakes. *Hydrobiologia*, *744*(1), 1–14. https://doi.org/10.1007/s10750-014-2050-y

Hamme R.C. & Emerson S.R. (2004) The solubility of neon, nitrogen and argon in distilled water and seawater. *Deep-Sea Research Part I-Oceanographic Research Papers,* **51,** 1517-1528. https://doi.org/10.1016/j.dsr.2004.06.009

Hassen A., Saidi N., Cherif M. & Boudabous A. (1998) Resistance of environmental bacteria to heavy metals. *Bioresource technology,* **64,** 7-15. https://doi.org/10.1016/S0960-8524(97)00161-2

Hessen, D. O., Håll, J. P., Thrane, J.-E., & Andersen, T. (2017). Coupling dissolved organic carbon, CO2 and productivity in boreal lakes. *Freshwater Biology*, *62*(5), 945–953. https://doi.org/10.1111/fwb.12914

Hilgert, S., Scapulatempo Fernandes, C. V., & Fuchs, S. (2019). Redistribution of methane emission hot spots under drawdown conditions. *Science of The Total Environment*, *646*, 958–971. https://doi.org/10.1016/j.scitotenv.2018.07.338

Horvatić J. & Peršić V. (2007) The effect of Ni 2+, Co 2+, Zn 2+, Cd 2+ and Hg 2+ on the growth rate of marine diatom Phaeodactylum tricornutum Bohlin: microplate growth inhibition test. *Bulletin of Environmental Contamination and Toxicology,* **79,** 494-498. https://doi.org/10.1007/s00128-007-9291-7

Houle, D., Augustin, F., & Couture, S. (2022). Rapid improvement of lake acid–base status in Atlantic Canada following steep decline in precipitation acidity. *Canadian Journal of Fisheries and Aquatic Sciences*, *79*(12), 2126–2137. https://doi.org/10.1139/cjfas-2021-0349

IEA. (2020). *Key World Energy Statistics 2020*. IEA, International Energy Agency. https://www.iea.org/reports/key-world-energy-statistics-2020

Jeffrey, L. C., Santos, I. R., Tait, D. R., Makings, U., & Maher, D. T. (2018). Seasonal Drivers of Carbon Dioxide Dynamics in a Hydrologically Modified Subtropical Tidal River and Estuary (Caboolture River, Australia). *Journal of Geophysical Research: Biogeosciences*, *123*(6), 1827–1849. https://doi.org/10.1029/2017JG004023

Jonsson, A., Meili, M., Bergström, A.-K., & Jansson, M. (2001). Whole-lake mineralization of allochthonous and autochthonous organic carbon in a large humic lake (örträsket, N. Sweden). *Limnology and Oceanography*, *46*(7), 1691–1700. https://doi.org/10.4319/lo.2001.46.7.1691

Karlsson, J., Giesler, R., Persson, J., & Lundin, E. (2013). High emission of carbon dioxide and methane during ice thaw in high latitude lakes. *Geophysical Research Letters*, *40*(6), Article 6. https://doi.org/10.1002/grl.50152

Khwaja, A. R., Bloom, P. R., & Brezonik, P. L. (2006). Binding Constants of Divalent Mercury (Hg2+) in Soil Humic Acids and Soil Organic Matter. *Environmental Science & Technology*, *40*(3), 844–849. https://doi.org/10.1021/es051085c

Kim, D., Mahabadi, N., Jang, J., & van Paassen, L. A. (2020). Assessing the Kinetics and Pore-Scale Characteristics of Biological Calcium Carbonate Precipitation in Porous Media using a Microfluidic Chip Experiment. *Water Resources Research*, *56*(2), e2019WR025420. https://doi.org/10.1029/2019WR025420

Klaus, M. (2023). Decadal increase in groundwater inorganic carbon concentrations across Sweden. *Communications Earth & Environment*, *4*(1), Article 1. https://doi.org/10.1038/s43247-023-00885-4

Kling, G. W., Kipphut, G. W., & Miller, M. C. (1991). Arctic Lakes and Streams as Gas Conduits to the Atmosphere: Implications for Tundra Carbon Budgets. *Science*, *251*(4991), 298–301. https://doi.org/10.1126/science.251.4991.298

Knowles, R. (1982). Denitrification. *Microbiological Reviews*, *46*(1), 43–70. https://doi.org/10.1128/mr.46.1.43-70.1982

Kokic, J., Wallin, M. B., Chmiel, H. E., Denfeld, B. A., & Sobek, S. (2015). Carbon dioxide evasion from headwater systems strongly contributes to the total export of carbon from a small boreal lake catchment. *Journal of Geophysical Research: Biogeosciences*, *120*(1), 13–28. https://doi.org/10.1002/2014JG002706

Koschorreck, M., Prairie, Y. T., Kim, J., & Marcé, R. (2021). Technical note: CO_2 is not like CH_4 – limits of and corrections to the headspace method to analyse pCO_2 in fresh water. *Biogeosciences*, *18*(5), 1619–1627. https://doi.org/10.5194/bg-18-1619-2021

Larrañaga, M., Lewis, R., & Lewis, R. (2016). Hawley's Condensed Chemical Dictionary, Sixteenth Edition. i–xiii. https://doi.org/10.1002/9781119312468.fmatter

Liang X., Lu X., Zhao J., Liang L., Zeng E.Y. & Gu B. (2019) Stepwise reduction approach reveals mercury competitive binding and exchange reactions within natural organic matter and mixed organic ligands. *Environmental Science & Technology,* **53,** 10685-10694. https://doi.org/10.1021/acs.est.9b02586

Machado Damazio, J., Cordeiro Geber de Melo, A., Piñeiro Maceira, M. E., Medeiros, A., Negrini, M., Alm, J., Schei, T. A., Tateda, Y., Smith, B., & Nielsen, N. (2012). *Guidelines for quantitative analysis of net GHG emissions from reservoirs: Volume 1: Measurement Programmes and Data Analysis*. International Energy Agency (IEA). https://www.ieahydro.org/media/992f6848/GHG_Guidelines_22October2012_Final.pdf

Magen, C., Lapham, L. L., Pohlman, J. W., Marshall, K., Bosman, S., Casso, M., & Chanton, J. P. (2014). A simple headspace equilibration method for measuring dissolved methane. Limnology and Oceanography: Methods, 12(9), 637–650. https://doi.org/10.4319/lom.2014.12.637

Miller, C. L., Southworth, G., Brooks, S., Liang, L., & Gu, B. (2009). Kinetic Controls on the Complexation between Mercury and Dissolved Organic Matter in a Contaminated Environment. *Environmental Science & Technology*, *43*(22), 8548–8553. https://doi.org/10.1021/es901891t

Millero F.J., Huang F. & Laferiere A.L. (2002) Solubility of oxygen in the major sea salts as a function of concentration and temperature. *Marine Chemistry,* **78,** 217-230. https://doi.org/10.1016/S0304-4203(02)00034-8

Myrstener, M., Fork, M. L., Bergström, A.-K., Puts, I. C., Hauptmann, D., Isles, P. D. F., Burrows, R. M., & Sponseller, R. A. (2022). Resolving the Drivers of Algal Nutrient Limitation from Boreal to Arctic Lakes and Streams. *Ecosystems*, *25*(8), 1682–1699. https://doi.org/10.1007/s10021-022-00759-4

Mørkved, P. T., Dörsch, P., & Bakken, L. R. (2007). The N2O product ratio of nitrification and its dependence on long-term changes in soil pH. *Soil Biology and Biochemistry*, *39*(8), 2048–2057. https://doi.org/10.1016/j.soilbio.2007.03.006

NILU. (2022). *EBAS*. https://ebas-data.nilu.no/Default.aspx

Nowack, B., Krug, H. F., & Height, M. (2011). 120 Years of Nanosilver History: Implications for Policy Makers. Environmental Science & Technology, 45(4), 1177–1183. https://doi.org/10.1021/es103316q

NPIRS. (2023). *Purdue University.* https://www.npirs.org/public

Okuku, E. O., Bouillon, S., Tole, M., & Borges, A. V. (2019). Diffusive emissions of methane and nitrous oxide from a cascade of tropical hydropower reservoirs in Kenya. *Lakes & Reservoirs: Science, Policy and Management for Sustainable Use*, *24*(2), 127–135. https://doi.org/10.1111/lre.12264

Parkhurst, D. L., & Appelo, C. A. J. (2013). *Description of input and examples for PHREEQC version 3—A computer program for speciation, batch-reaction, one-dimensional transport, and inverse geochemical calculations: U.S. Geological Survey Techniques and Methods* (book 6, chap. A43; p. 497). USGS. http://pubs.usgs.gov/tm/06/a43/

Powell K.J., Brown P.L., Byrne R.H., Gajda T., Hefter G., Sjöberg S. & Wanner H. (2004) Chemical speciation of Hg (II) with environmental inorganic ligands. *Australian Journal of Chemistry,* **57,** 993-1000. https://doi.org/10.1071/CH04063

Rai L.C., Gaur J.P. & Kumar H.D. (1981) Phycology and heavy-metal pollution. *Biological Reviews,* **56,** 99-151. https://doi.org/10.1111/j.1469-185X.1981.tb00345.x

Ratte, H. T. (1999). Bioaccumulation and toxicity of silver compounds: A review. *Environmental Toxicology and Chemistry*, *18*(1), 89–108. https://doi.org/10.1002/etc.5620180112

Ray, R., Miyajima, T., Watanabe, A., Yoshikai, M., Ferrera, C. M., Orizar, I., Nakamura, T., San Diego-McGlone, M. L., Herrera, E. C., & Nadaoka, K. (2021). Dissolved and particulate carbon export from a tropical mangrove-dominated riverine system. *Limnology and Oceanography*, *66*(11), 3944–3962. https://doi.org/10.1002/lno.11934

Rees, A. P., Brown, I. J., Jayakumar, A., Lessin, G., Somerfield, P. J., & Ward, B. B. (2021). Biological nitrous oxide consumption in oxygenated waters of the high latitude Atlantic Ocean. *Communications Earth & Environment*, *2*(1), Article 1. https://doi.org/10.1038/s43247-021-00104-y

Rippner, D. A., Margenot, A. J., Fakra, S. C., Aguilera, L. A., Li, C., Sohng, J., Dynarski, K. A., Waterhouse, H., McElroy, N., Wade, J., Hind, S. R., Green, P. G., Peak, D., McElrone, A. J., Chen, N., Feng, R., Scow, K. M., & Parikh, S. J. (2021). Microbial response to copper oxide nanoparticles in soils is controlled by land use rather than copper fate. *Environmental Science: Nano*, *8*(12), 3560–3576. https://doi.org/10.1039/D1EN00656H

Rohrlack T., Frostad P., Riise G. & Hagman C.H.C. (2020) Motile phytoplankton species such as Gonyostomum semen can significantly reduce CO_2 emissions from boreal lakes. *Limnologica,* **84,** 125810. https://doi.org/10.1016/j.limno.2020.125810

Schubert, C. J., Diem, T., & Eugster, W. (2012). Methane Emissions from a Small Wind Shielded Lake Determined by Eddy Covariance, Flux Chambers, Anchored Funnels, and Boundary Model Calculations: A Comparison. *Environmental Science & Technology*, *46*(8), 4515–4522. https://doi.org/10.1021/es203465x

Seitzinger, S. P. (1988). Denitrification in freshwater and coastal marine ecosystems: Ecological and geochemical significance. *Limnology and Oceanography*, *33*(4part2), 702–724. https://doi.org/10.4319/lo.1988.33.4part2.0702

Silver S. & Phung L.T. (2005) A bacterial view of the periodic table: genes and proteins for toxic inorganic ions. *Journal of Industrial Microbiology & Biotechnology,* **32,** 587-605. https://doi.org/10.1007/s10295-005-0019-6

Skjelkvåle, B. L., & de Wit, H. A. (2011). Trends in precipitation chemistry, surface water chemistry and aquatic biota in acidified areas in Europe and North America from 1990 to 2008 (ICP

912 Waters report 106/2011). In *126*. Norsk institutt for vannforskning.
913 https://niva.brage.unit.no/niva-xmlui/handle/11250/215591
914 Skyllberg, U. (2008). Competition among thiols and inorganic sulfides and polysulfides for Hg and
915 MeHg in wetland soils and sediments under suboxic conditions: Illumination of controversies
916 and implications for MeHg net production. *Journal of Geophysical Research:*
917 *Biogeosciences*, *113*(G2). https://doi.org/10.1029/2008JG000745
918 Sobek, S., Algesten, G., Bergström, A.-K., Jansson, M., & Tranvik, L. J. (2003). The catchment and
919 climate regulation of pCO2 in boreal lakes. *Global Change Biology*, *9*(4), 630–641.
920 https://doi.org/10.1046/j.1365-2486.2003.00619.x
921 Stumm W. & Morgan J.J. (1981) *Aquatic Chemistry. An introduction emphasizing chemical*
922 *equilibria in natural waters,* Wiley Interscience, New York.
923 Stumm, W., & Morgan, J. J. (1996). *Aquatic chemistry: Chemical equilibria and rates in natural*
924 *waters* (3rd ed.). Wiley.
925 Taipale S.J. & Sonninen E. (2009) The influence of preservation method and time on the delta C-13
926 value of dissolved inorganic carbon in water samples. *Rapid Communications in Mass*
927 *Spectrometry,* **23,** 2507-2510. https://doi.org/10.1002/rcm.4072
928 Takahashi H.A., Handa H., Sugiyama A., Matsushita M., Kondo M., Kimura H. & Tsujimura M.
929 (2019) Filtration and exposure to benzalkonium chloride or sodium chloride to preserve water
930 samples for dissolved inorganic carbon analysis. *Geochemical Journal,* **53,** 305-318.
931 https://doi.org/10.2343/geochemj.2.0570
932 Thottathil, S. D., Reis, P. C. J., & Prairie, Y. T. (2019). Methane oxidation kinetics in northern
933 freshwater lakes. *Biogeochemistry*, *143*(1), Article 1. https://doi.org/10.1007/s10533-019-
934 00552-x
935 Tipping E. (2007) Modelling the interactions of Hg(II) and methylmercury with humic substances
936 using WHAM/Model VI. *Applied Geochemistry,* **22,** 1624-1635.
937 Tørseth, K., Aas, W., Breivik, K., Fjæraa, A. M., Fiebig, M., Hjellbrekke, A. G., Lund Myhre, C.,
938 Solberg, S., & Yttri, K. E. (2012). Introduction to the European Monitoring and Evaluation
939 Programme (EMEP) and observed atmospheric composition change during
940 1972–2009. *Atmospheric Chemistry and Physics*, *12*(12), 5447–5481.
941 https://doi.org/10.5194/acp-12-5447-2012
942 Ullmann, F., Gerhartz, W., Yamamoto, Y. S., Campbell, F. T., Pfefferkorn, R., & Rounsaville, J. F.
943 (1985). Ullmann's encyclopedia of industrial chemistry (5th, completely rev. ed ed.). VCH.
944 UNESCO/IHA. (2008). *Assessment of the GHG status of freshwater reservoirs: Scoping paper*
945 (IHP/GHG-WG/3; p. 28). UNESCO/IHA, International Hydropower Association -
946 International Hydrological Programme, Working Group on Greenhouse Gas Status of
947 Freshwater Reservoirs. https://unesdoc.unesco.org/ark:/48223/pf0000181713
948 UNESCO/IHA. (2010). *GHG Measurement Guidelines for Freshwater Reservoirs* (p. 154).
949 UNESCO/IHA, International Hydropower Association.
950 https://www.hydropower.org/publications/ghg-measurement-guidelines-for-freshwater-
951 reservoirs
952 Urabe, J., Iwata, T., Yagami, Y., Kato, E., Suzuki, T., Hino, S., & Ban, S. (2011). Within-lake and
953 watershed determinants of carbon dioxide in surface water: A comparative analysis of a
954 variety of lakes in the Japanese Islands. *Limnology and Oceanography*, *56*(1), 49–60.
955 https://doi.org/10.4319/lo.2011.56.1.0049
956 Vachon, D., & Prairie, Y. T. (2013). The ecosystem size and shape dependence of gas transfer
957 velocity versus wind speed relationships in lakes. *Canadian Journal of Fisheries and Aquatic*
958 *Sciences*, *70*(12), Article 12. https://doi.org/10.1139/cjfas-2013-0241
959 Valiente, N., Eiler, A., Allesson, L., Andersen, T., Clayer, F., Crapart, C., Dörsch, P., Fontaine, L.,
960 Heuschele, J., Vogt, R., Wei, J., de Wit, H. A., & Hessen, D. O. (2022). *Catchment properties*
961 *as predictors of greenhouse gas concentrations across a gradient of boreal lakes*.
962 *10*(880619). https://doi.org/10.3389/fenvs.2022.880619
963 Valinia, S., Englund, G., Moldan, F., Futter, M. N., Köhler, S. J., Bishop, K., & Fölster, J. (2014).
964 Assessing anthropogenic impact on boreal lakes with historical fish species distribution data
965 and hydrogeochemical modeling. *Global Change Biology*, *20*(9), 2752–2764.
966 https://doi.org/10.1111/gcb.12527

van Grinsven, S., Oswald, K., Wehrli, B., Jegge, C., Zopfi, J., Lehmann, M. F., & Schubert, C. J. (2021). Methane oxidation in the waters of a humic-rich boreal lake stimulated by photosynthesis, nitrite, Fe(III) and humics. *Biogeosciences*, *18*(10), 3087–3101. https://doi.org/10.5194/bg-18-3087-2021

Wanninkhof, R. (2014). Relationship between wind speed and gas exchange over the ocean revisited. *Limnology and Oceanography: Methods*, *12*(6), Article 6. https://doi.org/10.4319/lom.2014.12.351

Webb, J. R., Santos, I. R., Maher, D. T., Macdonald, B., Robson, B., Isaac, P., & McHugh, I. (2018). Terrestrial versus aquatic carbon fluxes in a subtropical agricultural floodplain over an annual cycle. *Agricultural and Forest Meteorology*, *260–261*, 262–272. https://doi.org/10.1016/j.agrformet.2018.06.015

Weiss R.F. & Price B.A. (1980) Nitrous oxide solubility in water and seawater. *Marine Chemistry,* **8,** 347-359. https://doi.org/10.1016/0304-4203(80)90024-9

Weyhenmeyer, G. A., Hartmann, J., Hessen, D. O., Kopáček, J., Hejzlar, J., Jacquet, S., Hamilton, S. K., Verburg, P., Leach, T. H., Schmid, M., Flaim, G., Nõges, T., Nõges, P., Wentzky, V. C., Rogora, M., Rusak, J. A., Kosten, S., Paterson, A. M., Teubner, K., … Zechmeister, T. (2019). Widespread diminishing anthropogenic effects on calcium in freshwaters. *Scientific Reports*, *9*(1), Article 1. https://doi.org/10.1038/s41598-019-46838-w

Wilhelm E., Battino R. & Wilcock R.J. (1977) Low-pressure solubility of gases in liquid water. *Chemical Reviews,* **77,** 219-262. https://doi.org/10.1021/cr60306a003

Wilson J., Munizzi J. & Erhardt A.M. (2020) Preservation methods for the isotopic composition of dissolved carbon species in non-ideal conditions. *Rapid Communications in Mass Spectrometry,* **34**. https://doi.org/10.1002/rcm.8903

Xiao, S., Yang, H., Liu, D., Zhang, C., Lei, D., Wang, Y., Peng, F., Li, Y., Wang, C., Li, X., Wu, G., & Liu, L. (2014). Gas transfer velocities of methane and carbon dioxide in a subtropical shallow pond. *Tellus B: Chemical and Physical Meteorology*, *66*(1), 23795. https://doi.org/10.3402/tellusb.v66.23795

Xu F.F. & Imlay J.A. (2012) Silver(I), Mercury(II), Cadmium(II), and Zinc(II) Target Exposed Enzymic Iron-Sulfur Clusters when They Toxify Escherichia coli. *Applied and Environmental Microbiology,* **78,** 3614-3621. https://doi.org/10.1128/aem.07368-11

Yamamoto S., Alcauskas J.B. & Crozier T.E. (1976) Solubility of methane in distilled water and seawater. *Journal of Chemical and Engineering Data,* **21,** 78-80. https://doi.org/10.1021/je60068a029

Yan, F., Sillanpää, M., Kang, S., Aho, K. S., Qu, B., Wei, D., Li, X., Li, C., & Raymond, P. A. (2018). Lakes on the Tibetan Plateau as Conduits of Greenhouse Gases to the Atmosphere. *Journal of Geophysical Research: Biogeosciences*, *123*(7), 2091–2103. https://doi.org/10.1029/2017JG004379

Yang H., Andersen T., Dorsch P., Tominaga K., Thrane J.E. & Hessen D.O. (2015) Greenhouse gas metabolism in Nordic boreal lakes. *Biogeochemistry,* **126,** 211-225. https://doi.org/10.1007/s10533-015-0154-8

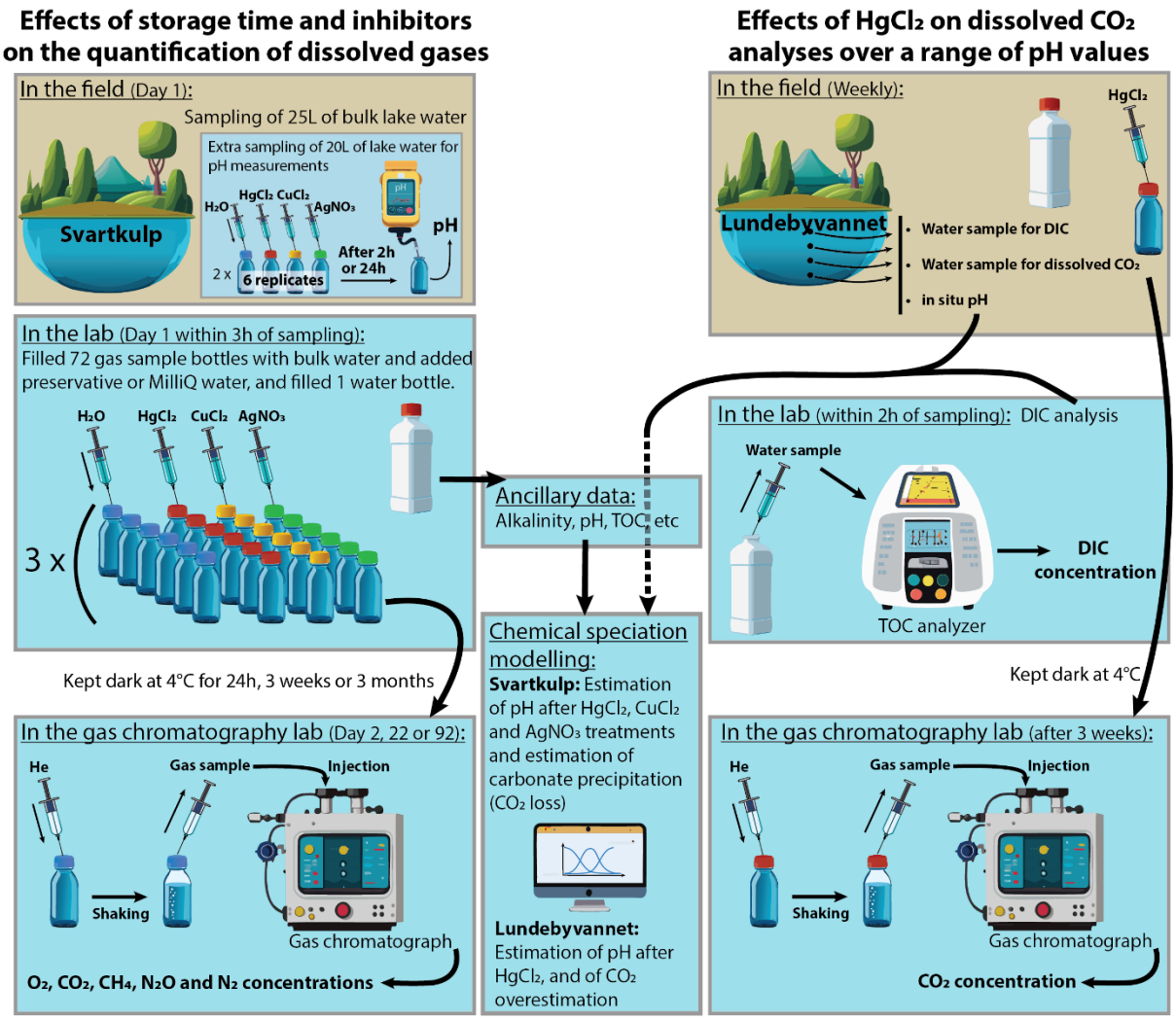

Fig. 1. Overview of experimental procedures. Several graphic items in this figure have been generated with the help of Adobe® Firefly™ Artificial Intelligence generator.

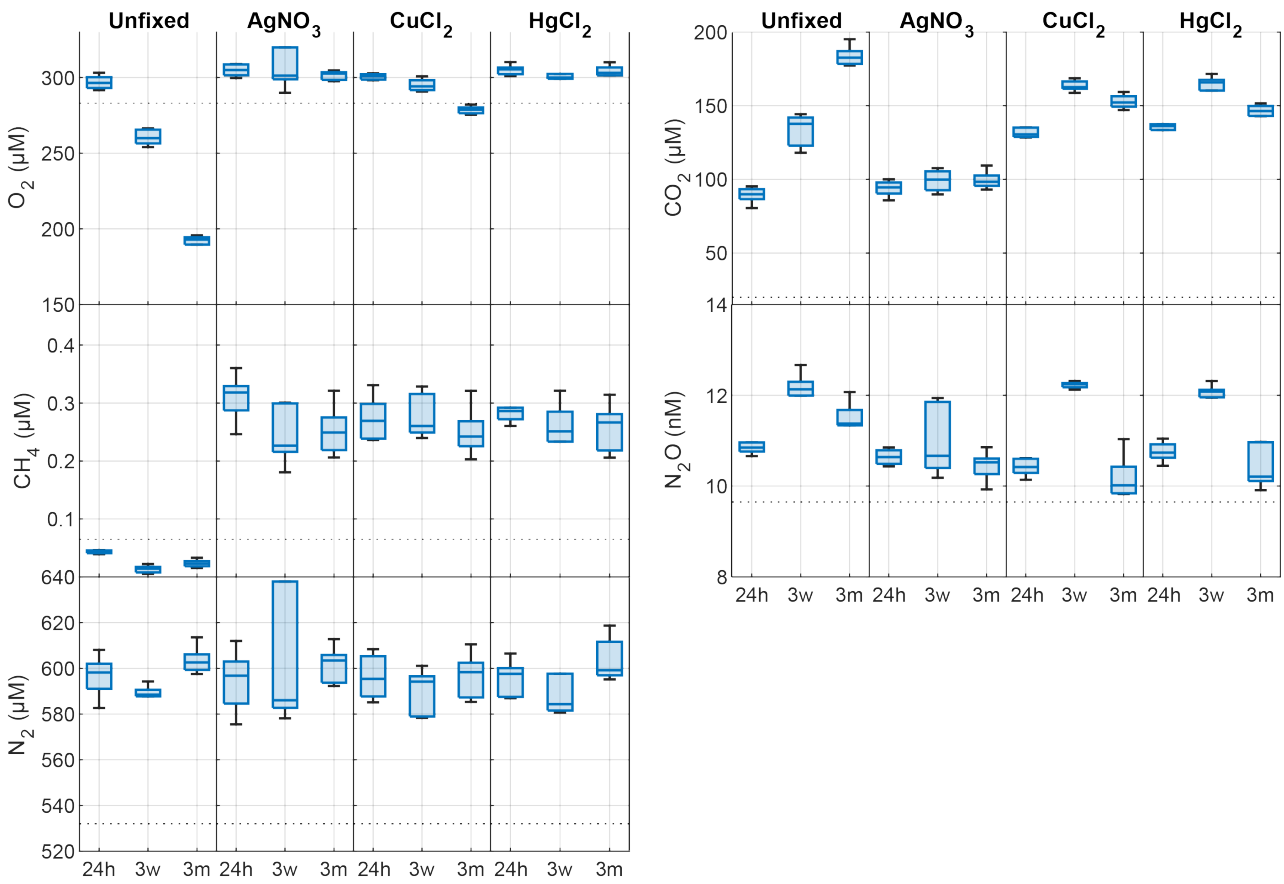

Fig 2. Changes in dissolved O_2, CO_2, CH_4, N_2O and N_2 concentrations (nM or µM) in the absence (unfixed) and presence of different preservatives ($AgNO_3$, $CuCl_2$, $HgCl_2$) at three times (24h, 24h after incubation start; 3w, three weeks after collection; 3m, three months after collection). The horizontal dotted line is the saturated gas concentration corresponding to 100% gas saturation at *in situ* lake temperature. Box plots show the median, 25th and 75th percentiles and the whiskers display minimum and maximum.

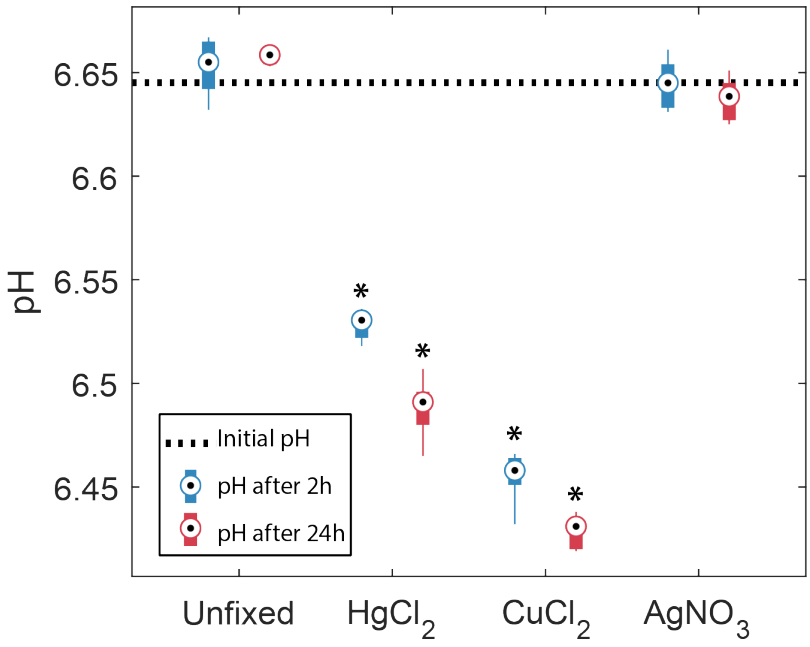

Fig 3. Observed changes in pH in the absence (unfixed) and presence of different preservatives ($AgNO_3$, $CuCl_2$, $HgCl_2$) at two times, 2h and 24h after the start of the incubation. The horizontal dotted line represents the initial pH of the bulk water sample. Box plots show the median, 25th and 75th percentiles and the whiskers display minimum and maximum of the 6 replicates. Stars indicate groups that are significantly different from each other and from the initial pH (two-way ANOVA).

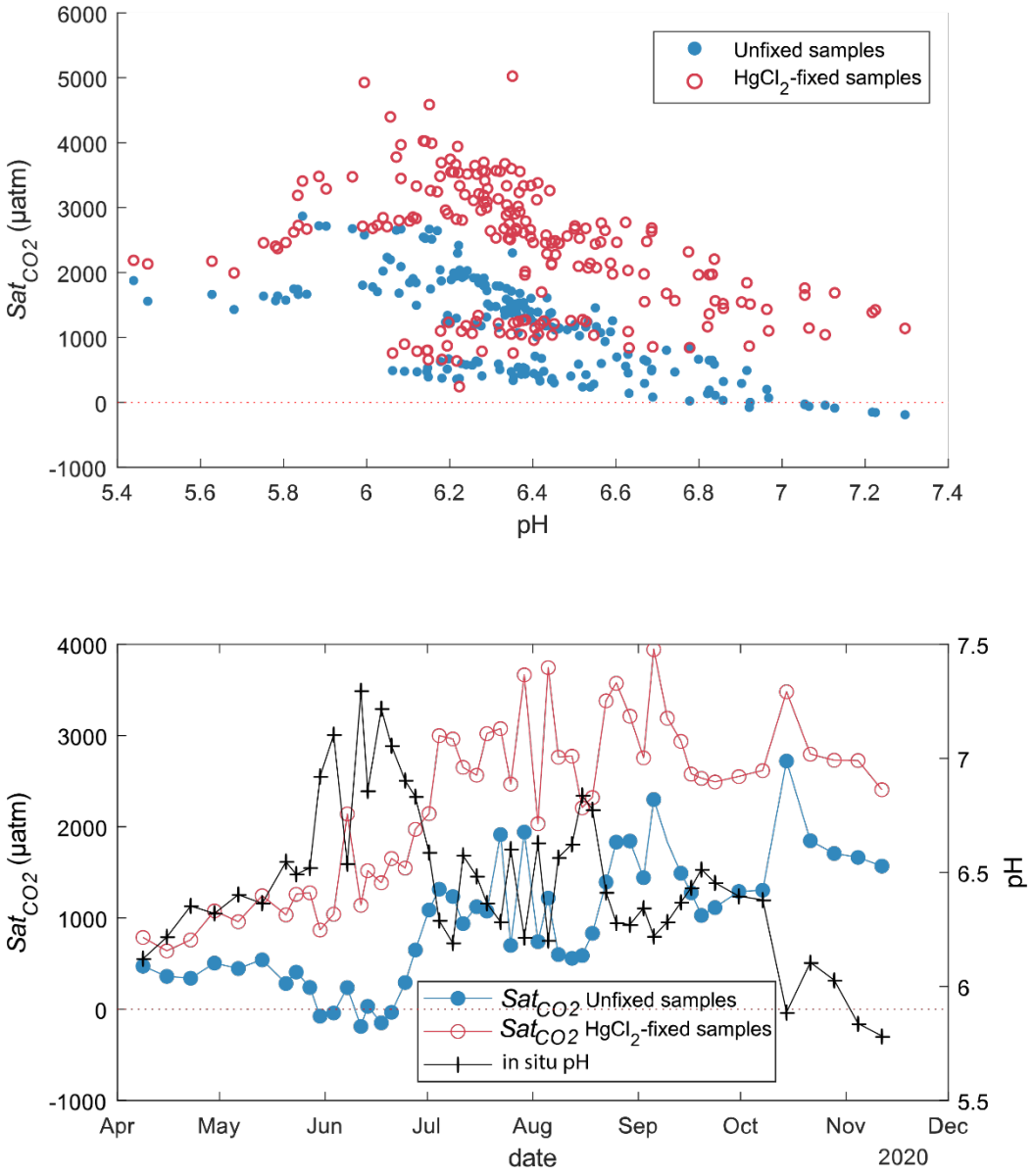

Fig. 4. CO_2 saturation deficit (Sat_{CO2}) in Lake Lundebyvannet as a function of in situ pH for all unfixed (obtained from DIC analysis) and $HgCl_2$-fixed (obtained from GC analysis) samples (top panel). Timeseries of pH and CO_2 saturation deficit of surface water (1-m deep) for unfixed and $HgCl_2$-fixed samples (bottom panel).

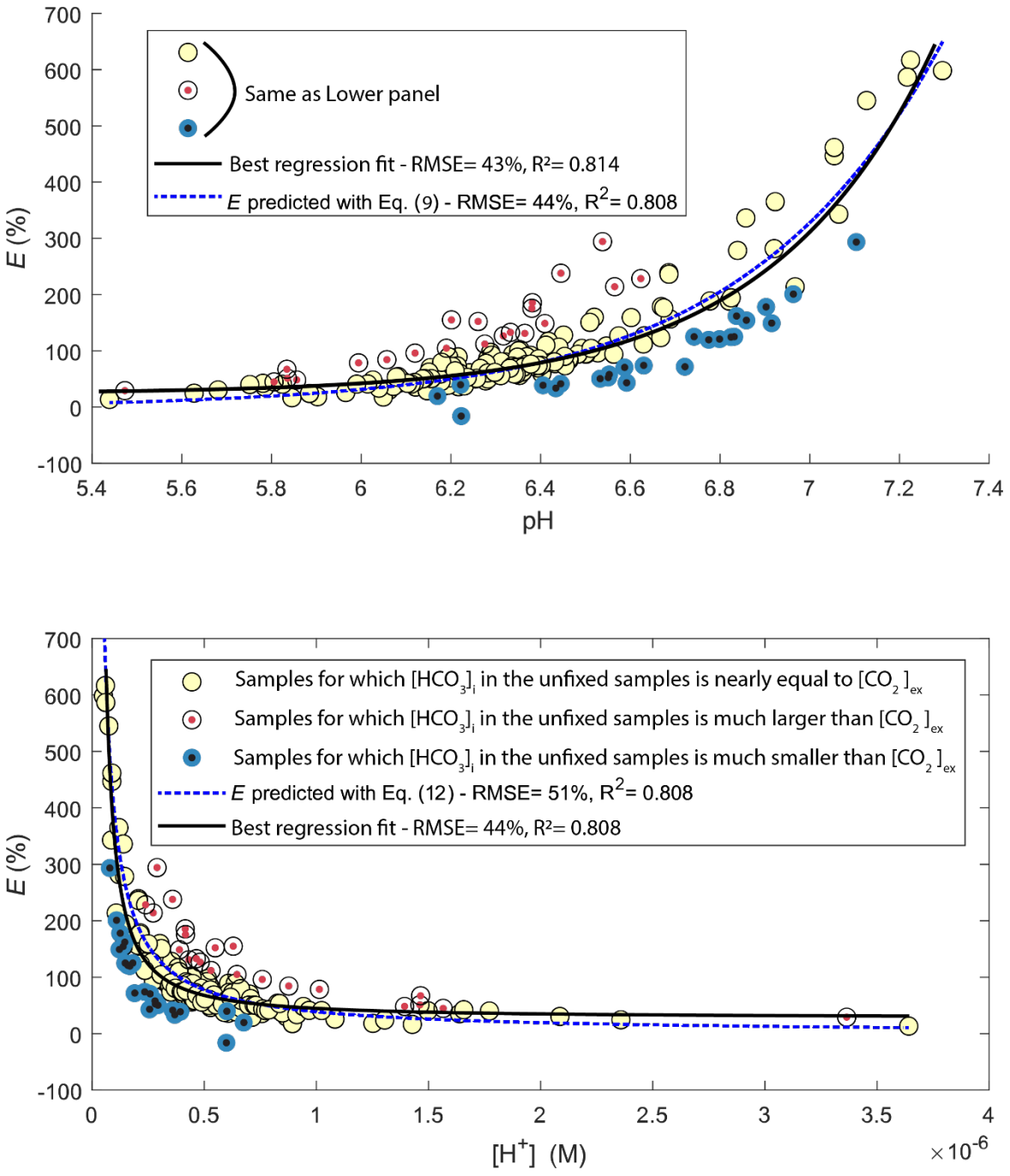

Fig. 5. Comparison of observed (circles) and predicted (blue line) relative overestimation (E) of CO_2 concentrations caused by $HgCl_2$ fixation in Lake Lundebyvannet samples as a function of pH (top panel) or proton concentration (bottom panel). The black line shows the best fit of the regression analysis. White symbols represent samples for which the bicarbonate concentration in the unfixed samples ($[HCO_3^-]_i$) is nearly equal to CO_2 overestimation ($[CO_2]_{ex}$), i.e., ± 20µM (equivalent to a pH error of 0.05), while red and blue symbols represent samples for which initial bicarbonate concentration was lower and higher than the CO_2 overestimation, respectively.

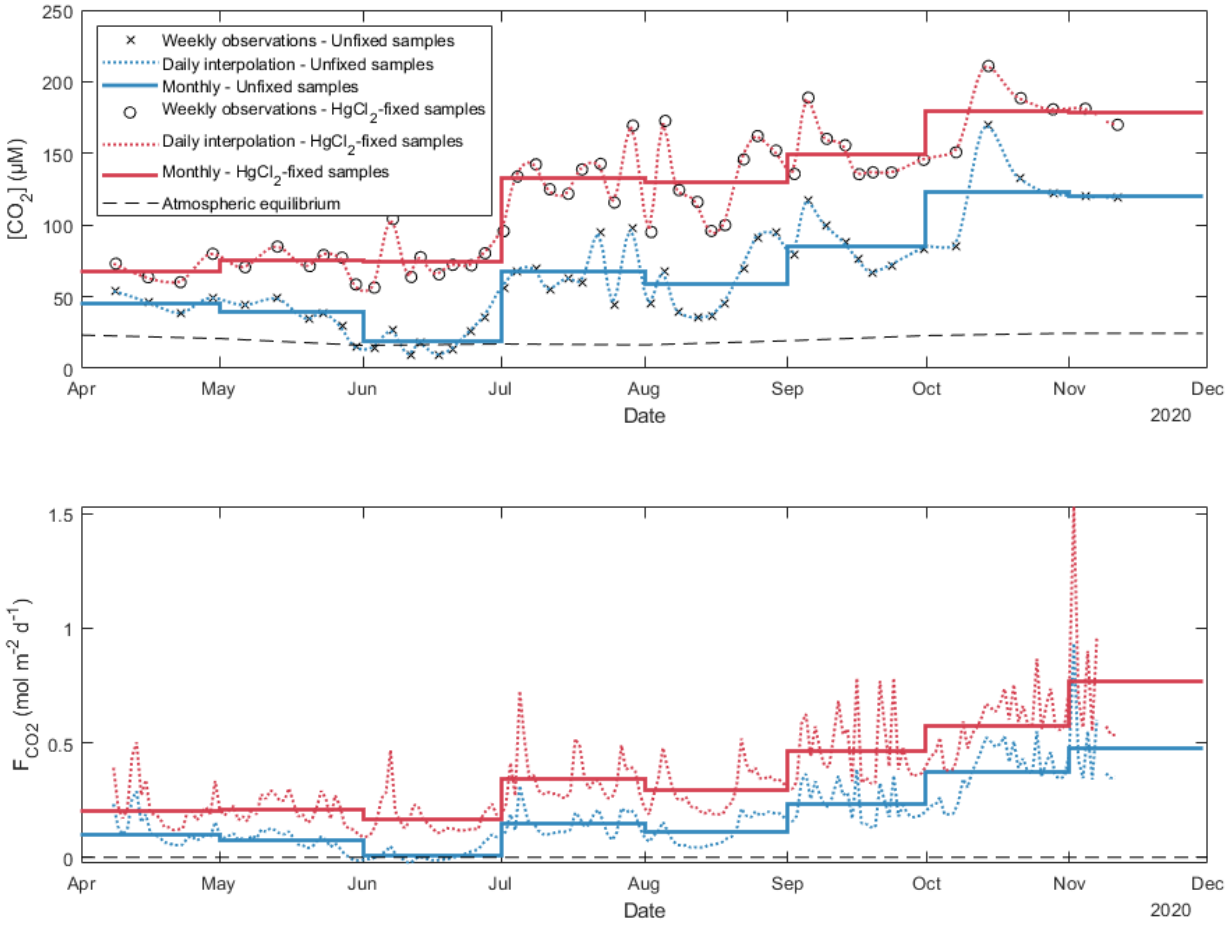

Fig. 6. Daily and monthly surface CO_2 concentrations ([CO_2]; top panel) and diffusion fluxes (F_{CO2}; bottom panel) at the water-atmosphere interface from Lake Lundebyvannet (also in Tab. 3). Unfixed samples were obtained by DIC analysis. Daily [CO_2] was interpolated from weekly data using a modified spline (see text for details). Diffusion fluxes were calculated following Cole & Caraco (1998).

Tab. 1. Stock and sample concentrations of $HgCl_2$, $CuCl_2$ and $AgNO_3$.

Salt	Stock solution	Sample concentration	Rationale
$HgCl_2$	70 g/L (saturated)	14.0±0.01 µg/mL (51.6 µM)	Dickson, Sabine & Christian, 2007
$CuCl_2$	131.9 g/L	26.4±0.02 µg/mL (154.7 µM)	3 × Hg
$AgNO_3$	87.6 g/L	17.5±0.02 µg/mL (103.1 µM)	2 × Hg

Tab. 2. pH and saturation indices of selected carbonate minerals estimated by PHREEQC for the unpreserved and preserved samples

Preservatives	pH	Saturation indices			
		$HgCO_3$	$Cu_2(OH)_2CO_3$ - Malachite	$Cu_2(OH)_2CO_3$ - Azurite	Ag_2CO_3
Unfixed	6.72	-2.31	-4.96	-8.71	-16.42
$HgCl_2$	6.40	3.64	-5.89	-10.10	-17.20
$CuCl_2$	6.45	-2.55	2.26	2.11	-17.44
$AgNO_3$	6.71	-2.31	-4.97	-8.73	-4.33

Tab. 3. CO_2 concentrations ($[CO_2]$, µM) and diffusion fluxes (F_{CO2}, mol m^{-2} d^{-1}) from Lake Lake Lundebyvannet estimated from $HgCl_2$-fixed and unfixed samples following Cole and Caraco (1998). Ice-free season spans April to November. Data are also shown in Fig. 6.

Preservatives		Apr.	May	Jun.	Jul.	Aug.	Sep.	Oct.	Nov.	Ice-free season
$[CO_2]$	None	45	39	19	68	59	85	123	120	67
	$HgCl_2$	68	75	74	133	130	149	179	178	121
	Diff (%)	+50	+93	+296	+96	+119	+75	+45	+49	+82
F_{CO2}	None	0.10	0.07	0.01	0.15	0.11	0.23	0.37	0.48	0.17
	$HgCl_2$	0.20	0.21	0.16	0.34	0.29	0.47	0.57	0.77	0.35
	Diff (%)	+97	+188	+2163	+130	+162	+99	+55	+62	+108